Copy No. _____

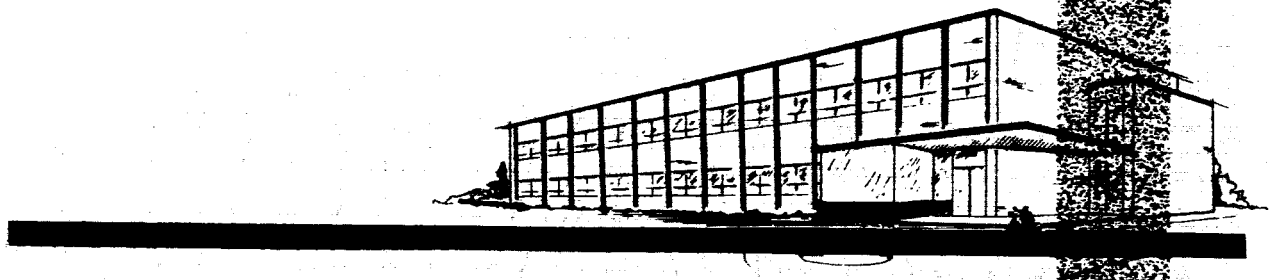

THE Bendix CORPORATION

BENDIX SYSTEMS DIVISION • ANN ARBOR MICHIGAN

OTS PRICE

XEROX $ 7.60 ph

MICROFILM $ _____

DOCKING STUDY
FINAL SUMMARY REPORT
BSR 933

June 12, 1964

Submitted to:

George C. Marshall Space Flight Center
National Aeronautics and Space Administration
Huntsville, Alabama

Attention: M-P&C-MPS

Contract NAS 8-5425

Period Covered:
17 June 1963 to 12 June 1964

THE BENDIX CORPORATION
BENDIX SYSTEMS DIVISION
Ann Arbor, Michigan

Authors: A. J. Besonis
S. I. Lieberman
W. G. Green

ABSTRACT

27906

The analytical formulation of the optimum (minimum fuel consumption) solution for docking with an earth satellite is described. This formulation is based on the use of calculus of variations and includes the equations for target and chaser motion, the Euler-Lagrange equations, boundary conditions and corner conditions. All equations are developed in three dimensions. The solution of a two-dimensional set is described based on the use of an idealized two-impulse transfer to establish a starting point for the iteration process.

Author

TABLE OF CONTENTS

LIST OF ILLUSTRATIONS

1.0 INTRODUCTION AND SUMMARY

ABST

This study describes the use of calculus of variations for obtaining fuel optimum rendezvous trajectories in order to accomplish docking between a chaser vehicle and an earth satellite. Docking is defined as that part of the mission which extends from chaser acquisition of the satellite to actual achievement of the rendezvous. The complete three dimensional mathematical formulation is defined. The calculus of variations model used is based on the problem of Lagrange and includes the equations of motion for target and chaser vehicle, the Euler-Lagrange equations, boundary and corner conditions.

A two dimensional model was derived on the basis of the three dimensional model and implemented on a digital computer. The initial values of the Lagrange multipliers were selected based upon the solution of an idealized two-impulse transfer. These multipliers yield satisfactory intercepts of the target for various selected intercept times. Due to the sensitivity of the multipliers, the definition of the thrust needed at intercept in order to match velocities and yield a truly optimum solution required a prohibitive amount of computation time. For example, an error in the seventh significant place of the switching function changed miss distance by approximately 200 feet. It is also shown below that fuel consumption is very insensitive to intercept time. These results are due to the type of trajectories flown. The target vehicle is in a circular orbit, and the eccentricity of the chaser orbit is on the order of 10^{-4}. Thus, the relative velocities at intercept are almost negligible.

2.0 PROBLEM FORMULATION

Mathematical formulation of the docking problem was accomplished in two parts: (1) the derivation of the equations of motion for the target and chaser, and (2) the development of the Euler Lagrange equations and transversality conditions for the variational problem (optimization). These analyses are discussed separately below.

2.1 EQUATIONS OF MOTION

The equations of motion for the target and chaser are derived in Appendix A in terms of "state variables" ($x, y, \dot{x}, \dot{y}$, etc.) for two coordinate references. One coordinate reference, designated as the x, y, z system,

is an earth-centered inertial set with the y axis along the local vertical at the initial condition point; the x axis along the horizontal of the launch plane at the initial point, and the z axis completing a right-handed set. The other coordinate reference, is an instantaneous set, centered in the chaser with the y axis along the longitudinal axis of the chaser; the x and z axis are chosen so that the resulting coordinate system is parallel to the inertial set initially. These equations of motion are based upon the following model:

1. Spherical earth
2. Inverse gravity law
3. The only forces acting on the chaser are thrust and gravity
4. The only force acting on the target is gravity
5. Rotation effects on chaser are ignored
6. Constant fuel burning rate
7. The center of mass of the chaser is fixed with respect to the chaser
8. The target is in a non-impacting, low altitude earth orbit
9. The chaser is initially in a near-identical orbit to that of the target.

The equations defining the motion of the target moving in an elliptic trajectory over a spherical earth are written in the inertial coordinate system with the six orbital elements (semi-major axis, eccentricity, etc.) as parameters. Since these equations cannot be readily solved for the state variable ($x, \dot{x}, y, \dot{y}$, etc.) an iterative procedure based on a Taylor series expansion is defined for computing the state variables as a function of time.

The equations defining the motion of the chaser are written with the constraint that the thrust vector lies along the chaser longitudinal axis only.

2.2 THE VARIATIONAL PROBLEM

The Euler-Lagrange equations for the variational problem are developed in Appendix B, using minimization of fuel consumption as the optimizing criteria. The equations are constrained by the condition that the mass flow rate is bounded by maximum and minimum values; and that optimum solutions consist only of subarcs of maximum and minimum mass flow rates. The switching condition is derived along with the relationship between the thrust vector and the inertial coordinates.

The fourteen first order differential equations defining the problem require 15 boundary conditions for their solution, since the intercept time is not defined. These boundary condition are defined in Appendix B, in terms of state variable notation, for the desired terminal conditions of the docking problem. The Erdmann-Weierstrass corner conditions, and the Weierstrass condition for the existance of a minimal value are also applied to the problem.

3.0 COMPUTER FEASIBILITY SOLUTION

The feasibility of the complete three dimensional formulation, discussed above, was checked by simplifying the formulation, implementing the resulting equations on a digital computer, and computing trial solutions. The simplified formulation involves a two dimensional model (chaser and target coplanar) with the target in a circular orbit; the equations for this simplified formulation are given in Appendix C.

In order to obtain the trial solutions, it is necessary to determine initial conditions for the Lagrange multipliers. Since, for large thrust/mass ratios, the optimum trajectory will be close to an idealized two-impulse transfer, the two impulse transfer was solved to obtain initial estimates for the Lagrange multipliers. A Runge-Kutta iterative technique can be used to converge the solutions from the initial estimates to the desired values, assuming the initial estimates are sufficiently accurate to allow convergence.

As described in Appendix C, an investigation was carried out on the effect of the initial conditions in the Lagrange multipliers on intercept. The results of this investigation indicated that the fuel consumption required for the two-impulse transfer was very insensitive to intercept time;

conversely, very small variations in the magnitude and direction of the velocity impulses have very large effects on the rendezvous point. This implies that the initial values of the Lagrange multipliers are similarly sensitive in the non-impulse transfer. This was demonstrated for the following specific case:

Target altitude	=	200 n mi.
Thrust	=	30,000 lb.
Specific impulse	=	440 sec.
Initial chaser altitude	=	374.0 km
Initial chaser velocity magnitude	=	6.98 km/sec.
Initial chaser flight path angle	=	-1.40 deg.
Initial central angle between chaser and target	=	1 deg.

First of all, a value of $\eta_0 = 1.38291$ (Initial thrust direction) was found from the impulsive transfer solution. Variations in the multiplier $\dot{\eta}_0$ were studied in terms of its effect on changes in the intercept position. These results are shown in Figure 1. The extreme sensitivity of intercept position to $\dot{\eta}_0$ is immediately obvious.

On the basis of computer runs of this type, initial values of the multipliers may be chosen and used for the computation of the rendezvous trajectories. These rendezvous trajectories are shown in relative coordinates in Figure 2. ξ and ζ are the position of the chaser relative to the intercept target position. The initial conditions are the same as for the previous figure. Only the trajectory near intercept is given. Two things should be noted. First of all, for a proper choice of the Lagrange multipliers found from the impulsive transfer case, miss distances may be made negligibly small. Secondly, a change in the seventh decimal place for the Lagrange Multiplier Γ_0 changes the miss distance from 20 to 270 feet, for this particular case. Therefore, any future changes in the multipliers in order to obtain true rendezvous (zero relative velocity) would be exceedingly difficult to perform. The use of the Runga-Kutta technique to obtain a convergent solution would be impractical.

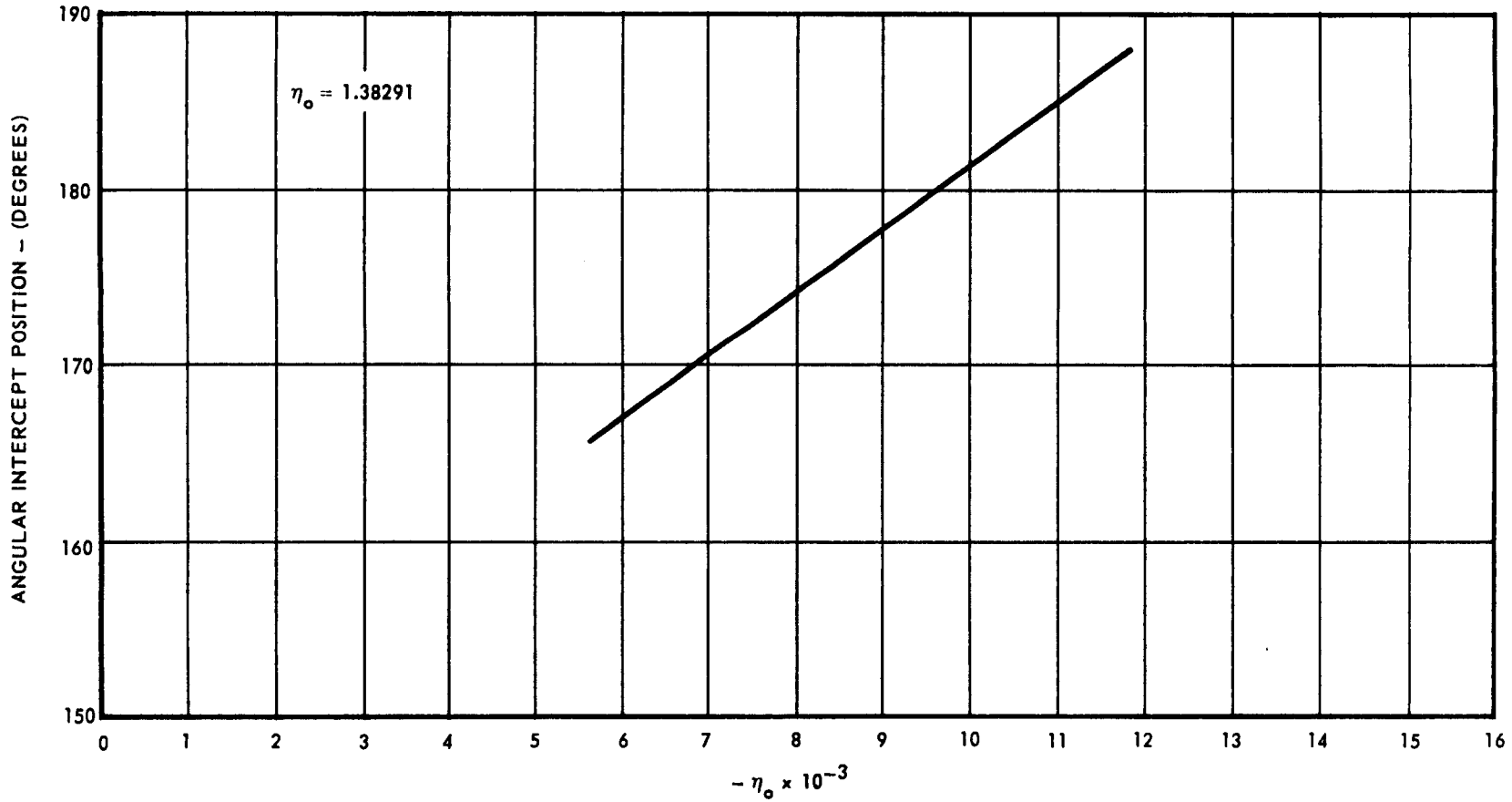

Figure 1 Angular intercept position of chaser as a function of $\dot{M}_o$

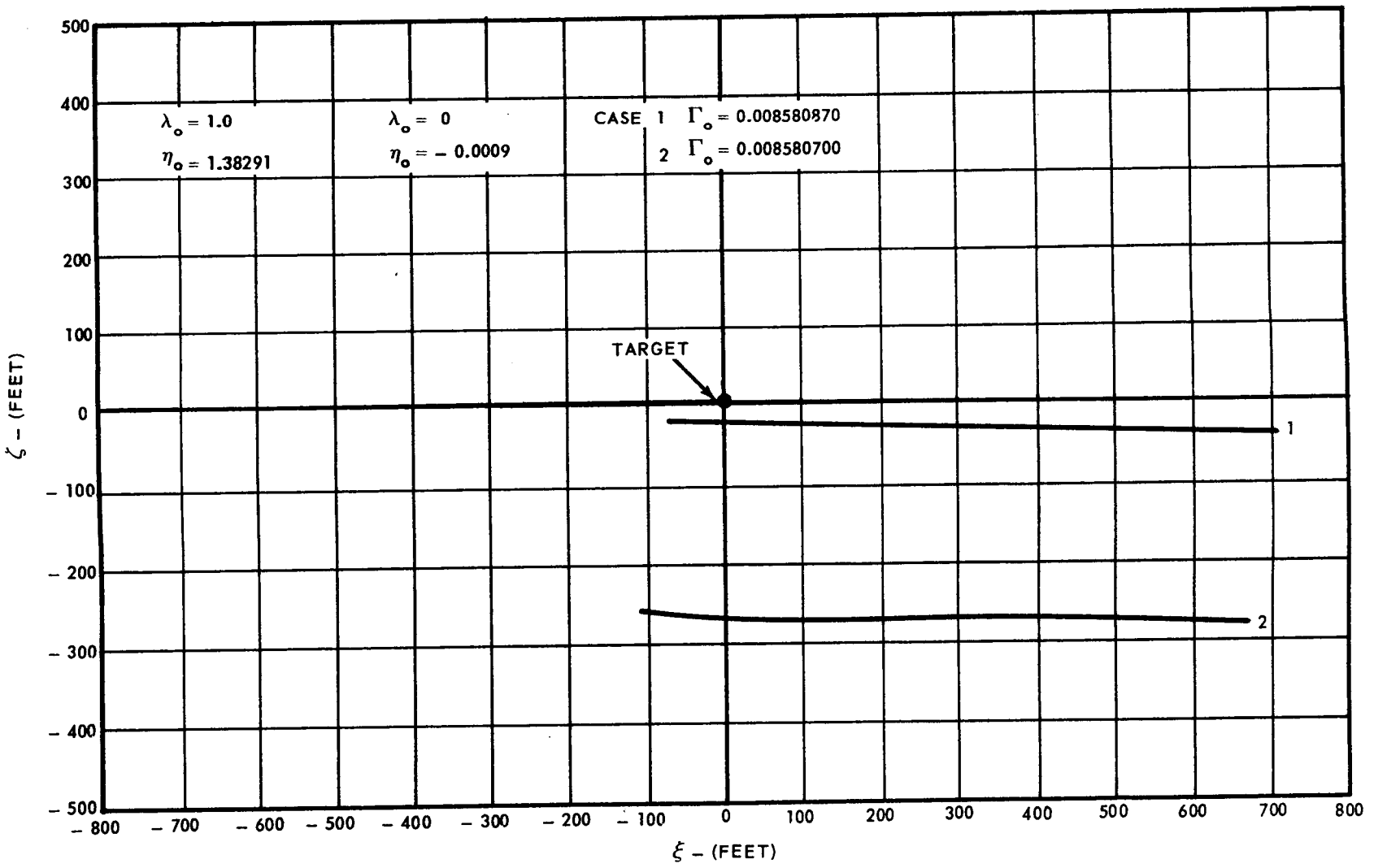

Figure 2 Rendezvous Trajectoris in Relative Coordinates

4.0 CONCLUSIONS

In the cases where the initial positions of target and chaser are close together and large thrusts are available, the two-impulse solution to the rendezvous trajectory provides a simpler solution than the calculus of variations model with negligible effect on fuel consumption. Furthermore, these cases are ones in which the boundary value problem becomes most difficult, since iterative procedures based on first order approximations to the Lagrange multiplier initial conditions are wholly inadequate unless the solution is essentially known to begin with. The Lagrange multiplier method becomes more significant as the initial orbital conditions become separated or the thrust levels become quite small.

Another possible approach to the problem would be to start with Equations (5-2) (Appendix C) as the equations of motion, with f set equal to zero, and derive the Euler-Lagrange equations accordingly. The resulting boundary-value problem may not be so critical, and hence, solvable by conventional methods.

APPENDIX A

CHASER AND TARGET EQUATIONS OF MOTION

1.0 INTRODUCTION

The equations of motion for the target and chaser are derived in this appendix. Section 2.0 defines the coordinate reference systems and the relationships between the coordinate systems. Section 3.0 defines the chaser equations, and Section 4.0 defines the target equations. Since the target equations cannot be readily solved for the state variables, an iterative procedure is defined in Section 5.0 for computing the state variables as a function of time.

2.0 REFERENCE SYSTEMS

2.1 PLUMBLINE SYSTEM

The plumbline system as shown in Figure A-1 has its origin at the center of the earth with the y axis parallel to the gravity gradient at the point of launch. Assuming a spherical earth and an inverse gravitational field, this axis passes through the point of launch. The x axis is parallel to the earth fixed chaser launch azimuth at the launch point. A right hand coordinate system is now formed by properly choosing the z-axis. This system is denoted by

$$\bar{x} = \begin{matrix} x \\ y \\ z \end{matrix}$$

2.2 CHASER VEHICLE SYSTEM

The chaser vehicle system of coordinates is defined by having its origin at the center of gravity of the chaser and the y_M axis along the longitudinal

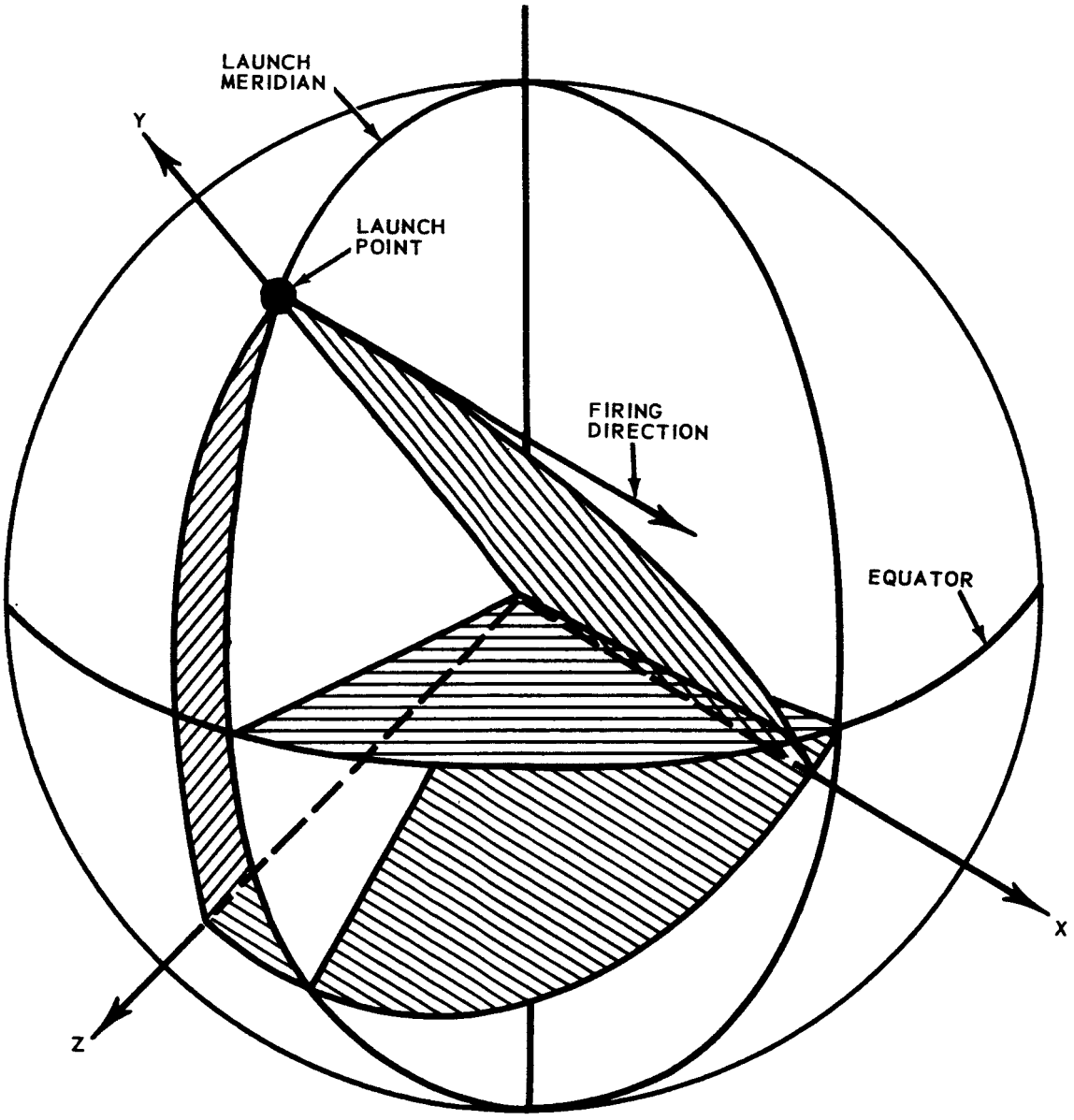

Figure A-1 Plumbline System

axis of the chaser as shown in Figure A-2. The x_M and z_M axes are chosen so that the resulting coordinate system is parallel to the plumbline system at launch. This system is denoted by

$$\bar{x}_M = \begin{matrix} x_M \\ y_M \\ z_M \end{matrix}$$

2.3 COORDINATE TRANSFORMATION

As the chaser moves in flight the two coordinate systems are related through pitch (χ_p), roll (χ_r), and yaw (χ_y). For the geometry of this study, this relationship is defined by the following transformation:

$$x = [A_\chi]^T \bar{x}_M$$

where

$$[A_\chi]^T = \begin{matrix} \cos\chi_p\cos\chi_r & -\sin\chi_p\cos\chi_y - \cos\chi_p\sin\chi_r\sin\chi_y & \sin\chi_p\sin\chi_y - \cos\chi_p\sin\chi_r\cos\chi_y \\ \sin\chi_p\cos\chi_r & \cos\chi_p\cos\chi_y - \sin\chi_p\sin\chi_r\sin\chi_y & -\cos\chi_p\sin\chi_y - \sin\chi_p\sin\chi_r\cos\chi_y \\ \sin\chi_r & \cos\chi_r\sin\chi_y & \cos\chi_r\cos\chi_y \end{matrix}$$

3.0 CHASER EQUATIONS OF MOTION

Considering the thrust in the x_M coordinate system,

$$F = \begin{matrix} 0 \\ F \\ 0 \end{matrix}$$

Newton's second law may be written in the form

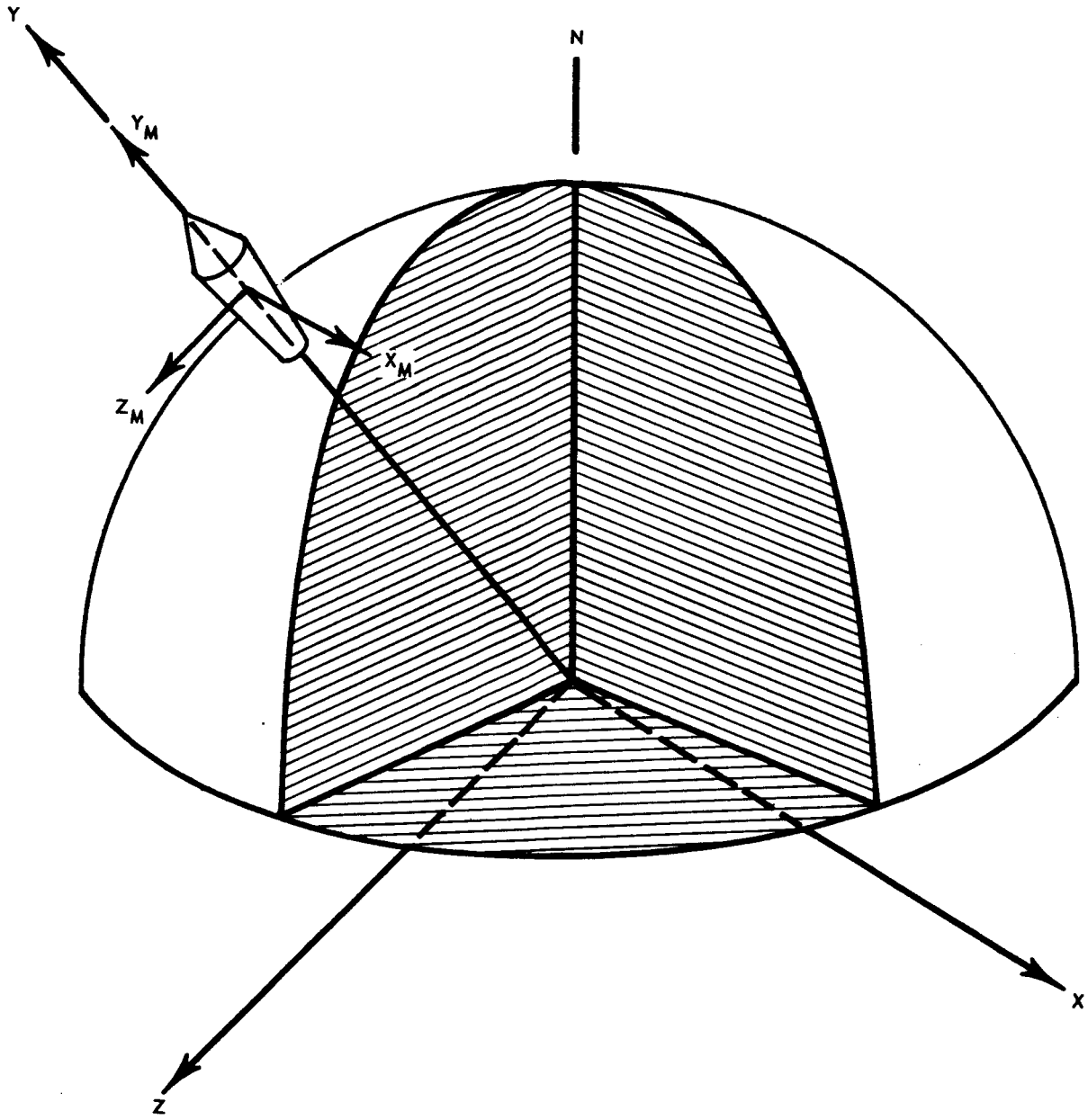

Figure A-2 Chaser Coordinate System

$$\ddot{\bar{x}} = \frac{1}{m_R}[A_\chi]^T \bar{F} + \ddot{\bar{x}}_g \qquad (3\text{-}1)$$

where

m_R = the mass of the chaser

$\ddot{\bar{x}}_g$ = the acceleration vector due to gravity

$\ddot{\bar{x}}$ = the total acceleration vector.

The acceleration components of Equation 3-1 are shown in Figure A-3. The problem formulation is based on the following assumptions:

1. Spherical earth
2. Inverse gravity law
3. The only forces acting on the chaser are thrust and gravity
4. Rotation effects on the chaser are ignored
5. Constant fuel burning rate
6. The center of mass of the chaser is fixed with respect to the chaser.

4.0 TARGET EQUATIONS OF MOTION

Given a target vehicle moving in the earth's central force field and a chaser vehicle ascending to dock with the target, the condition for docking requires that at the terminal point, the state variables of the chaser vehicle match those of the target. The purpose of this section is to develop the integrals of the target motion in the coordinate system chosen to describe the chaser motion. This coordinate system, designated as the x-y-z system is an earth-centered inertial set with the y axis along the local vertical of the launch site, at time of launch; the x asix along the horizontal of the launch plane at the launch site, and the z axis completing a right-handed set. In this earth-centered coordinate system, the target motion is given by

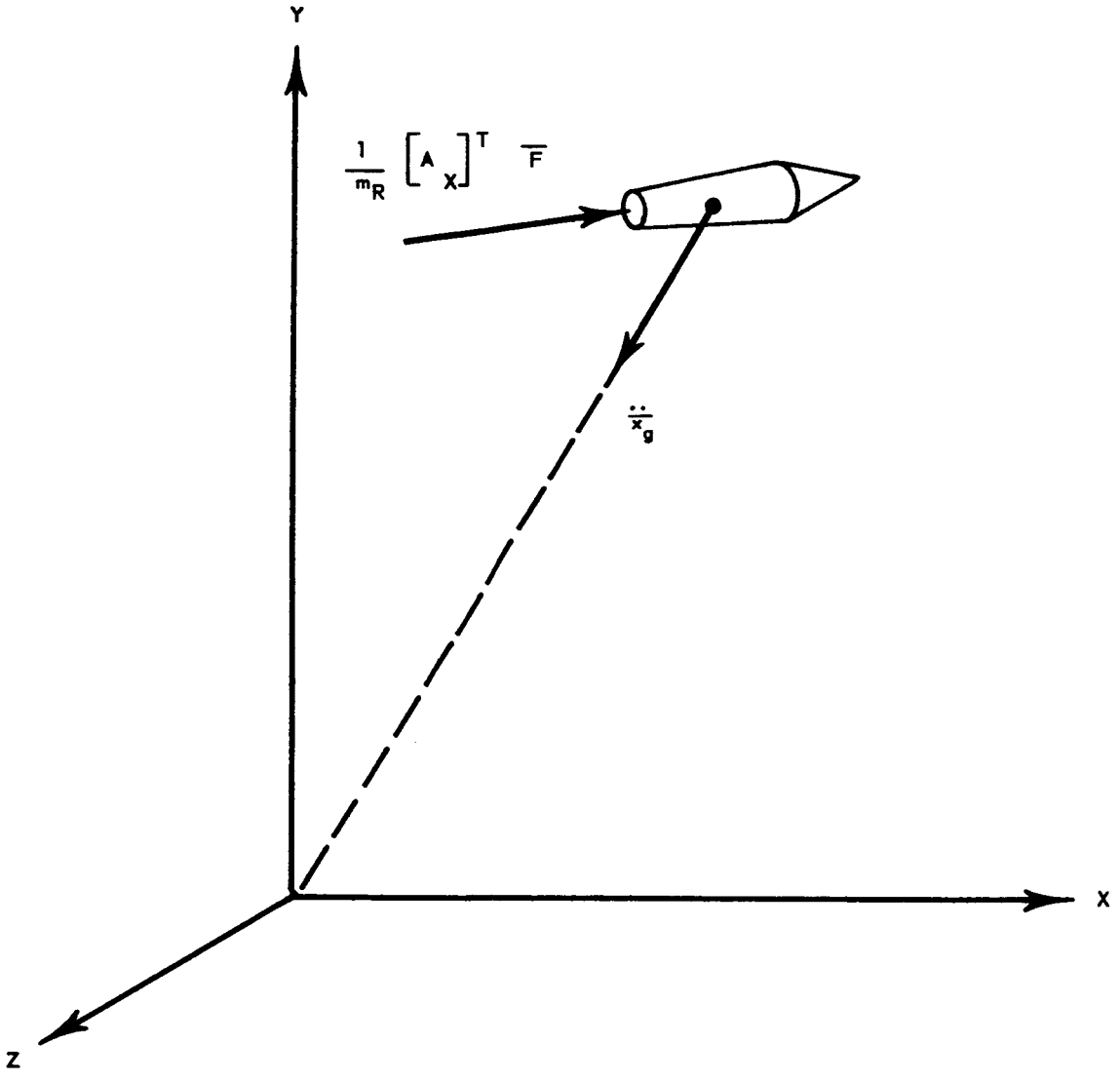

Figure A-3 Acceleration Components

$$\ddot{X} = -\frac{g_o R_E^2 X}{(X^2 + Y^2 + Z^2)^{3/2}} \tag{4-1}$$

$$\ddot{Y} = -\frac{g_o R_E^2 Y}{(X^2 + Y^2 + Z^2)^{3/2}} \tag{4-2}$$

$$\ddot{Z} = -\frac{g_o R_E^2 Z}{(X^2 + Y^2 + Z^2)^{3/2}} \tag{4-3}$$

where

g_o = the acceleration due to gravity at the earth's surface

R_E = the mean radius of the earth.

Define the potential function

$$U = \frac{g_o R_E^2}{(X^2 + Y^2 + Z^2)^{1/2}} \tag{4-4}$$

Now Equations (4-1), (4-2), and (4-3) can be written as

$$\ddot{X} = \frac{\partial U}{\partial X} \tag{4-5}$$

$$\ddot{Y} = \frac{\partial U}{\partial Y} \tag{4-6}$$

$$\ddot{Z} = \frac{\partial U}{\partial Z} \tag{4-7}$$

Multiplying these equations by $\dot{X}$, $\dot{Y}$, and $\dot{Z}$, respectively, and adding, yields

$$\dddot{X}\dot{X} + \dddot{Y}\dot{Y} + \dddot{Z}\dot{Z} = \dot{U}$$

The integral of this yields the well-known expression for the conservation of energy

$$1/2[\dot{(X)}^2 + \dot{(Y)}^2 + \dot{(Z)}^2] - \frac{g_o R_E^2}{(X^2 + Y^2 + Z^2)^{1/2}} = C_1$$

By taking the vector product of Equations (4-5), (4-6), and (4-7) with the vector $\vec{r} = \vec{i}X + \vec{j}Y + \vec{k}Z$ and observing the vector identity

$$\dot{\vec{r}} \times \dot{\vec{r}} = 0$$

three additional integrals are obtained:

$$\dot{Y}Z - Z\dot{Y} = C_2 \qquad (4\text{-}9)$$

$$\dot{Z}X - X\dot{Z} = C_3 \qquad (4\text{-}10)$$

$$\dot{X}Y - Y\dot{X} = C_4 \qquad (4\text{-}11)$$

It can readily be shown that Equations (4-9), (4-10), and (4-11) represent the other conservation law in component form, the conservation of angular momentum. To develop the remaining two integrals, it is observed first that by multiplying Equations (4-9), (4-10), and (4-11) by X, Y, and Z, respectively and adding, yields the equation

$$C_2X + C_3Y + C_4Z = 0 \qquad (4\text{-}12)$$

This equation states that the motion of the vehicle will be contained in a plane passing through the origin. It will prove convenient to define this plane by the following transformations:

$$\begin{pmatrix} x_1 \\ y_1 \\ z_1 \end{pmatrix} = \begin{pmatrix} \cos\Omega & 0 & -\sin\Omega \\ 0 & 1 & 0 \\ \sin\Omega & 0 & \cos\Omega \end{pmatrix} \begin{pmatrix} x \\ y \\ z \end{pmatrix}$$

$$\begin{pmatrix} x_2 \\ Y_2 \\ z_2 \end{pmatrix} = \begin{pmatrix} 1 & 0 & 0 \\ 0 & \cos\mu & \sin\mu \\ 0 & -\sin\mu & \cos\mu \end{pmatrix} \begin{pmatrix} x_1 \\ Y_1 \\ z_1 \end{pmatrix}$$

The combined transformation matrix becomes

$$\begin{pmatrix} x \\ Y \\ z \end{pmatrix} = \begin{pmatrix} \cos\Omega & \sin\mu\sin\Omega & \cos\mu\sin\Omega \\ 0 & \cos\mu & -\sin\mu \\ -\sin\Omega & \sin\mu\cos\Omega & \cos\mu\cos\Omega \end{pmatrix} \begin{pmatrix} x_2 \\ Y_2 \\ z_2 \end{pmatrix} \quad (4\text{-}13)$$

It is noted that when the ferry is launched exactly into the target plane of motion, both angles Ω and μ are zero, otherwise the target moves in the x_2 - y_2 plane. Thus the total angular momentum vector is along the z_2 axis. Using the transformation (4-13), the components of angular momentum C_2, C_3, and C_4 in Equations (4-9), (4-10), and (4-11), become

$$\left.\begin{aligned} C_2 &= h\cos\mu\sin\Omega \\ C_3 &= h\sin\mu \\ C_4 &= h\cos\mu\cos\Omega \end{aligned}\right\} \quad (4\text{-}14)$$

where h is the angular momentum of the target.

The target motion can be described in polar coordinates by rotating the x_2 and y_2 axes through an angle θ about the z_2 axis, such that the transformed axis x_3 is in the direction of the radius vector from the target.

This transformation is given by

$$\begin{pmatrix} x_3 \\ Y_3 \\ z_3 \end{pmatrix} = \begin{pmatrix} \cos\theta & \sin\theta & 0 \\ -\sin\theta & \cos\theta & 0 \\ 0 & 0 & 1 \end{pmatrix} \begin{pmatrix} x_2 \\ Y_2 \\ z_2 \end{pmatrix} \quad (4\text{-}15)$$

In the $x_2 - y_2 - z_2$ system, the angular momentum is given by

$$X_2\dot{Y}_2 - Y_2\dot{X}_2 = h \tag{4-16}$$

Using transformation (4-15), Equation (4-16) becomes

$$r^2\dot{\theta} = h \tag{4-17}$$

From geometry $r^2\dot{\theta}^2 = 2\dot{A}$

where A is the area swept out by the radius vector.

Integration of Equation (4-17) yields

$$2A = ht + C_5 \tag{4-18}$$

The remaining integral can be found from the energy integral, Equation (4-8), by writing it in polar coordinates (r, θ)

$$(\dot{r})^2 + r^2(\dot{\theta})^2 = \frac{2g_o R_E^2}{r} + C_1^1 \tag{4-19}$$

Where

$$C_1^1 = 2C_1$$

Since

$$\dot{r} = \dot{\theta}\,\frac{dr}{d\theta}$$

and from Equation (4-17)

$$\dot{\theta} = \frac{h}{r^2}.$$

Equation (4-19) can also be written

$$\left(\frac{dr}{d\theta}\right)^2 + r^2 = \frac{2g_o R_E^2 r^3}{h^2} + \frac{C_1^1 r^4}{h^2} \tag{4-20}$$

Solving this for $\frac{dr}{d\theta}$ and separating variables

$$d\theta = \frac{-d\left(h/r\right)}{\left[C_1 + \frac{g_o^2 R_E^2}{h^2} - \left(\frac{g_o R_E^2}{h}\,\frac{h}{r}\right)^2\right]^{1/2}}$$

Integrating this

$$\theta = \cos^{-1}\left(u/B\right) + \theta_o \qquad (4\text{-}21)$$

where

$$-u = \frac{g_o R_E^2}{h} - \frac{h}{r}$$

and

$$B^2 = C_1 + \frac{g_o^2 R_E^4}{h^2}$$

Solving Equation (4-21) for r, the familiar equation for a conic in polar coordinates with the origin at one of the foci is obtained;

$$r = \frac{h^2/g_o R_E^2}{1 + \frac{C_1 h^2}{g_o^2 R_E^4} + 1\cos\left(\theta - \theta_o\right)} \qquad (4\text{-}22)$$

The form of this conic is determined by two constants of motion which are generally defined as

$$p = h^2/g_o R_E^2 \qquad \text{(semi-latus rectum)}$$

$$e = 1 + \frac{C_1 h^2}{g_o^2 R_E^4} \qquad \text{(eccentricity)}$$

The constant of integration is defined by

$$r = h^2/g_o R_E^2 = p \text{ when } \theta - \theta_o = \pi/2,$$

where θ_o denotes the orientation of the semi-major axis with respect to the x_2 axis.

Since the case of target motion in an elliptic trajectory is of interest, Equation (4-22) can be written in the rectangular coordinates x_o, y_o.

$$\frac{X_o^2}{a^2} + \frac{Y_o^2}{b^2} = 1 \qquad (4\text{-}23)$$

where a and b are the semi-major and semi-minor axes of the ellipse, respectively. If we arbitrarily choose the two constants of motion as a and e, Equation (4-23) becomes

$$\frac{X_o^2}{a^2} + \frac{Y_o^2}{a^2(1-e^2)} = 1 \qquad (4\text{-}24)$$

To write Equation (4-24) in the x-y-z system, it is noted that

$$X_o = X_2 \cos\theta_o + Y_2 \sin\theta_o$$

$$Y_o = -X_2 \sin\theta_o + Y_2 \cos\theta_o$$

and from the transformation (4-13)

$$X_2 = X \cos\Omega - Z \sin\Omega$$

$$Y_2 = X \sin\mu \sin\Omega + Y \cos\mu + Z \sin\mu \cos\Omega$$

Then,

$$X_o = (X \cos\Omega - Z \sin\_) \cos\theta_o + (X \sin\mu \sin\Omega + Y \cos\mu + Z \sin\mu \cos\Omega) \sin\theta_o$$

$$Y_o = -(X \cos\Omega - Z \sin\Omega) \sin\theta_o + (X \sin\mu \sin\Omega + Y \cos\mu + Z \sin\mu \cos\Omega) \cos\theta_o$$

Substituting these expressions into Equation (4-24), the trajectory becomes

$$\frac{1}{a^2}\Big[(X\cos\Omega - Z\sin\Omega)\cos\theta_o + (X\sin\mu\sin\Omega + Y\cos\mu + Z\sin\mu\cos\Omega)\sin\theta_o\Big]^2 + \frac{1}{a^2(1-e^2)}\Big[-(X\cos\Omega - Z\sin\Omega)\sin\theta_o + (X\sin\mu\sin\Omega + Y\cos\mu + Z\sin\mu\cos\Omega)\cos\theta_o\Big]^2 - 1 = 0 \qquad (4\text{-}25)$$

This is the equation for elliptic motion in the x, y, z coordinates.

To obtain integral (4-18) in terms of the x-y-z coordinates, consider the sketch shown in Figure A-4.

From the geometry,

$$\frac{\text{Area AFP}}{\text{Area ellipse}} = \frac{\text{Area AFQ}}{\text{Area circle}}$$

and

$$\overline{DA} = a(1-e) - X_o$$

To compute area AFQ, note:

$$\overline{DQ} = Y_o a/b$$

$$\text{Area FDQ} = \frac{1}{2} Y_o X_o \, a/b$$

$$\tan M = \frac{Y_o a/b}{ae + X_o}$$

$$\text{Area CAQ} = \frac{a^2 M}{2} = \frac{a^2}{2}\tan^{-1}\frac{Y_o a/b}{ae + X_o}$$

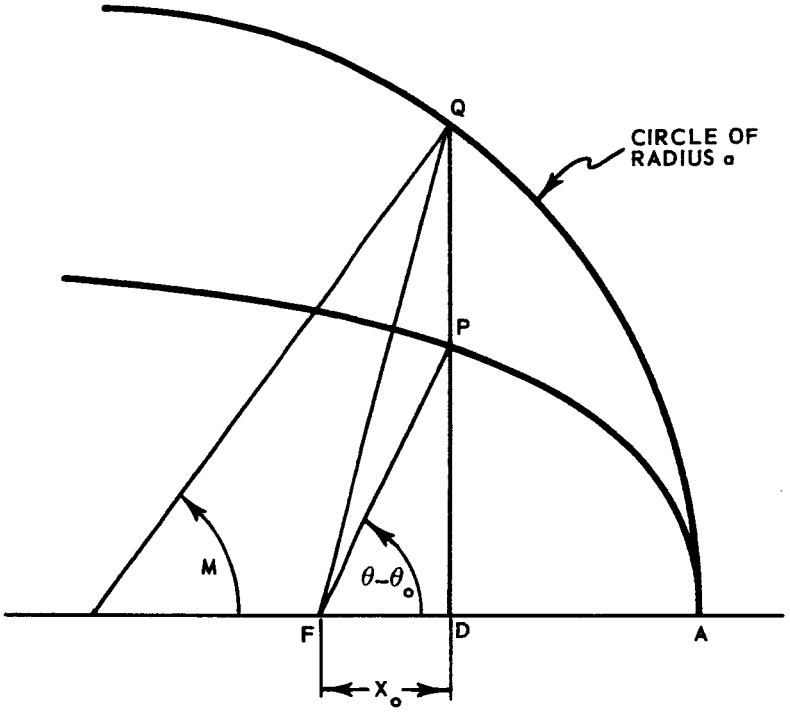

Figure A-4 Geometry of Target Orbit

$$\text{Area CDQ} = \frac{1}{2}\,(ae + X_o)\,Y_o\,a/b$$

$$\text{Area AFQ} = \text{Area CAQ} - \text{Area CDQ} + \text{Area FDQ}$$

Substituting from above

$$\text{Area AFQ} = \frac{a^2}{2}\left(\tan^{-1}\frac{Y_o/\sqrt{1-e^2}}{ae + X_o} - \frac{eY_o}{a\sqrt{1-e^2}}\right)$$

Then,

$$\text{Area AFP} = \frac{a^2\sqrt{1-e^2}}{2}\left(\tan^{-1}\frac{Y_o/\sqrt{1-e^2}}{ae + X_o} - \frac{eY_o}{a\sqrt{1-e^2}}\right)$$

After transforming coordinates, Area AFP can be written in terms of X and Y

$$\text{Area AFP} = \frac{a^2\sqrt{1-e^2}}{2}\tan^{-1}\frac{1}{\sqrt{1-e^2}}$$

$$X(\sin\mu\sin\Omega\cos\theta_o - \cos\mu\sin\theta_o) + Y\cos\mu\cos\theta_o + Z)\sin\mu\cos\Omega\cos\theta_o + \sin\Omega\sin\theta_o)$$

$$ae + X(\cos\Omega\cos\theta_o + \sin\mu\sin\Omega\sin\theta_o) + Y\cos\mu\sin\theta_o + Z(\sin\mu\cos\Omega\sin\theta_o - \sin\mu\cos\theta_o)$$

$$- \frac{e}{a\sqrt{1-e^2}}\left\{\left[X(\sin\mu\sin\Omega\cos\theta_o - \cos\Omega\sin\theta_o) + Y\cos\mu\cos\theta_o + Z(\sin\Omega\sin\theta_o + \sin\mu\cos\Omega\cos\theta_o)\right]\right\}$$

Substituting this into Equation (4-18) and noting that

$$h = R_E\sqrt{ag_o}\sqrt{1-e^2}$$

the final form of this integral becomes

$$a^2 \sqrt{1-e^2} \tan^{-1} \frac{1}{\sqrt{1-e^2}} \qquad (4\text{-}26)$$

$$\frac{X(\sin\mu \sin\Omega \cos\theta_o - \cos\Omega \sin\theta_o) - Y\cos\mu\cos\theta_o + Z(\sin\mu\cos\Omega\cos\theta_o + \sin\Omega\sin\theta_o)}{ae + X(\cos\Omega\cos\theta_o + \sin\mu\sin\Omega\sin\theta_o) + Y\cos\mu\sin\theta_o + Z(\sin\mu\cos\Omega\sin\theta_o - \sin\Omega\cos\theta_o)}$$

$$- \frac{e}{a\sqrt{1-e^2}} \left[X(\sin\mu\sin\Omega\cos\theta_o - \cos\Omega\sin\theta_o) + Y\cos\mu\cos\theta_o + Z(\sin\Omega\sin\theta_o + \sin\mu\cos\Omega\cos\theta_o) \right] = R_E \sqrt{ag_o}\sqrt{1-e^2}(t-\tau_p)$$

where τ_p is the time of perigee crossing.

Summarizing the results; for a target moving in an elliptic trajectory over a spherical earth with the trajectory defined by a, e, Ω, μ, θ_o, and τ, the following equations completely define the motion of the target in the chaser coordinates of the ferry:

$$\frac{1}{2}\left[(X)^2 + (\dot{Y})^2 + (\dot{Z})^2 \right] - \frac{\sqrt{g_o R_E^2}}{X^2 + Y^2 + Z^2} + \frac{g_o R_E^2}{2a} = 0 \qquad (4\text{-}27)$$

$$Y\dot{Z} - Z\dot{Y} - R_E\sqrt{ag_o}\sqrt{1-e^2}\cos\mu\sin\Omega = 0 \qquad (4\text{-}28)$$

$$\dot{Z}X - \dot{X}Z + R_E\sqrt{ag_o}\sqrt{1 - e^2}\sin\mu = 0 \tag{4-29}$$

$$\dot{X}Y - \dot{Y}X - R_E\sqrt{ag_o}\sqrt{1 - e^2}\cos\mu\cos\Omega + 0 \tag{4-30}$$

$$\begin{aligned}&\frac{1}{a^2}\Big[X(\cos\Omega\cos\theta_o + \sin\mu\sin\Omega\sin\theta_o) + Y\cos\mu\sin\theta_o \\ &\quad + Z(\sin\mu\cos\Omega\sin\theta_o - \sin\Omega\cos\theta_o)\Big]^2 \\ &+ \frac{1}{a^2(1 - e^2)}\Big[X(\sin\mu\sin\Omega\cos\theta_o - \cos\Omega\sin\theta_o) + Y\cos\mu\cos\theta_o \\ &\quad + Z(\sin\Omega\sin\theta_o + \sin\mu\cos\Omega\cos\theta_o)\Big]^2 - 1 = 0\end{aligned} \tag{4-31}$$

$$a^2\sqrt{1 - e^2}\quad \tan^{-1}\frac{1}{\sqrt{1 - e^2}} \tag{4-32}$$

$$\frac{X(\sin\mu\sin\Omega\cos\theta_o - \cos\Omega\sin\theta_o) - Y\cos\mu\cos\theta_o + Z(\sin\mu\cos\Omega\cos\theta_o + \sin\Omega\sin\theta_o)}{ae + X(\cos\Omega\cos\theta_o + \sin\mu\sin\Omega\sin\theta_o) + Y\cos\mu\sin\theta_o + Z(\sin\mu\cos\Omega\sin\theta_o - \sin\Omega\cos\theta_o)}$$

$$\begin{aligned}&-\frac{e}{a\sqrt{1 - e^2}}\Big[X(\sin\mu\sin\_\cos\theta_o - \cos\_\sin\theta_o) + Y\cos\mu\cos\theta_o + Z(\sin\Omega\sin\theta_o \\ &\quad + \sin\mu\cos\Omega\cos\theta_o)\Big] - R_E\sqrt{ag_o}\sqrt{1 - e^2}(t - t_p) = 0\end{aligned}$$

For the docking problem considered, these equations become the set of terminal conditions for the chaser.

5.0 SOLUTION FOR FINAL CONDITIONS

For the target orbit, orbits with very low eccentricities are considered. Furthermore, it is assumed that the angles Ω and μ are small. Since the Equations (4-27) through (4-32) cannot readily be solved for the state variables $\dot{X}$, $\dot{Y}$, $\dot{Z}$, X, Y, and Z, the circular orbit solution with $\Omega = 0$, and $\mu = 0$ is considered as the first approximation. Denoting this solution by barred quantities:

$$\bar{X} = \bar{r} \cos (\theta_o + \alpha) \tag{5-1}$$

$$\bar{Y} = \bar{r} \sin (\theta_o + \alpha) \tag{5-2}$$

$$\dot{\bar{X}} = \bar{V} \cos (\theta_o + \alpha) \tag{5-3}$$

$$\dot{\bar{Y}} = -\bar{V} \sin (\theta_o + \alpha)$$

$$\bar{Z} = 0$$

$$\dot{\bar{Z}} = 0$$

where the parameter α is specified (specified docking time) and is given by

$$\alpha = \frac{k}{a^{3/2}} t$$

$$k = g_o R_E^2$$

The parameters $\bar{r}$ and $\bar{V}$ can be considered as the mean orbital radius and the mean orbital velocity, respectively.

To obtain the exact solution, a linear iteration based on a Taylor series expansion is considered. Given a function

$$F = F(X_1, X_2, X_3, X_4, X_5, X_6) = 0,$$

its expansion about an approximate solution becomes

$$F(\bar{X}_1, \bar{X}_2, \bar{X}_3, \bar{X}_4, \bar{X}_5, \bar{X}_6)$$

$$+ \frac{\partial F}{\partial X_1} \Delta X_1 + \frac{\partial F}{\partial X_2} \Delta X_2 + \cdots\cdots + \frac{\partial F}{\partial X_6} \Delta X_6$$

$$+ \text{higher order terms} \approx 0$$

with the partial derivatives evaluated at $\bar{X}_1, \bar{X}_2, \cdots\cdots \bar{X}_6$.

For n simultaneous equations, considering only first order terms,

$$\begin{matrix} a_{11}\ a_{12}\ a_{13}\ a_{14}\ a_{15}\ a_{16} \cdots\cdots a_{1n} & & \Delta X_1 & & F_{10} \\ a_{21}\ a_{22} \cdots\cdots & & \Delta X_2 & & F_{20} \\ \cdots\cdots\cdots\cdots\cdots & & \cdots\cdots & = - & \cdots\cdots\cdots \\ a_{n1}\ a_{n2} \cdots\cdots & a_{nn} & \Delta X_n & & F_{no} \end{matrix}$$

where the coefficients a_{mn} are the partial derivatives evaluated at the approximate solution, and F_{no} denotes the function F_n evaluated at the approximate solution.

After obtaining the first solution from Equations (5-1) through (5-6), the solution would proceed by solving each iteration cycle for the changes ΔX_n.

For the six simultaneous equations considered, the coefficients a_{mn} are given by:

$$a_{11} = \frac{2k^2\overline{X}}{[\overline{X}^2 + \overline{Y}^2 + \overline{Z}^2]^{3/2}}$$

$$a_{12} = \frac{2k^2\overline{Y}}{[\overline{X}^2 + \overline{Y}^2 + \overline{Z}^2]^{3/2}}$$

$$a_{13} = \frac{2k^2\overline{Z}}{[\overline{X}^2 + \overline{Y}^2 + \overline{Z}^2]^{3/2}}$$

$$a_{14} = 2\overline{\dot{X}}$$

$$a_{15} = 2\overline{\dot{Y}}$$

$$a_{16} = 2\overline{\dot{Z}}$$

$$a_{21} = 0$$

$$a_{22} = \overline{Z}$$

$$a_{23} = -\overline{Y}$$

$$a_{24} = 0$$

$$a_{25} = -\overline{Z}$$

$$a_{26} = \overline{Y}$$

$$a_{31} = -\overline{Z}$$

$$a_{32} = 0$$

$$a_{33} = \overline{X}$$

$$a_{34} = \overline{Z}$$

$$a_{35} = 0$$

$$a_{36} = -\overline{X}$$

$$a_{41} = \overline{Y}$$

$$a_{42} = -\overline{X}$$

$$a_{43} = 0$$

$$a_{44} = -\overline{Y}$$

$$a_{45} = \overline{X}$$

$$a_{46} = 0$$

$$a_{51} = 2\{\overline{X}(\cos^2 \Omega + \sin^2 \mu \sin^2 \Omega) + \overline{Y} \cos \mu \sin \mu \sin \Omega$$
$$- \overline{Z} \sin \Omega \cos \Omega \cos^2 \mu + (e^2 + e^4)[\overline{X}(\cos \Omega \cos \theta_o$$
$$- \sin \mu \sin \Omega \sin \theta_o) - \overline{Y} \cos \mu \sin \theta_o - \overline{Z}(\sin \Omega \cos \theta_o$$
$$+ \sin \mu \cos \Omega \sin \theta_o)](\cos \Omega \cos \theta_o - \sin \mu \sin \Omega \sin \theta_o)\}$$

$$a_{52} = 2\{\overline{X}\sin\mu\ \sin\Omega\cos\mu + \overline{Y}\cos^2\mu + \overline{Z}\sin\mu\ \cos\Omega\cos\mu$$
$$- (e^2 + e^4)[\overline{X}(\cos\Omega\cos\theta_o - \sin\mu\ \sin\Omega\sin\theta_o)$$
$$- \overline{Y}\cos\mu\ \sin\theta_o - \overline{Z}(\sin\Omega\cos\theta_o + \sin\mu\ \cos\Omega\sin\theta_o)]\cos\mu\ \sin\theta_o\}$$

$$a_{53} = 2\{-\overline{X}\cos^2\mu\ \sin\Omega\cos\Omega + \overline{Y}\cos\mu\ \sin\mu\ \cos\Omega + \overline{Z}(\sin^2\Omega + \sin^2\mu\ \cos^2\Omega)$$
$$- (e^2 + e^4)[\overline{X}(\cos\Omega\cos\theta_o - \sin\mu\ \sin\Omega\sin\theta_o) - \overline{Y}\cos\mu\ \sin\theta_o$$
$$- \overline{Z}(\sin\Omega\cos\theta_o + \sin\mu\ \cos\Omega\sin\theta_o)](\sin\Omega\cos\theta_o + \sin\mu\ \cos\Omega\sin\theta_o)\}$$

$$a_{54} = 0$$

$$a_{55} = 0$$

$$a_{56} = 0$$

$$a_{61} = \frac{1}{\sqrt{1 - e^2}}[ae(\cos\Omega\cos\theta_o - \sin\mu\ \sin\Omega\sin\theta_o) + Y\cos\mu\ \cos\Omega$$
$$+ \overline{Z}\sin\mu\,][ae + \overline{X}(\cos\Omega\sin\theta_o + \sin\mu\ \sin\Omega\cos\theta_o)$$
$$+ \overline{Y}\cos\mu\ \cos\theta_o + \overline{Z}(\sin\mu\ \cos\Omega\cos\theta_o - \sin\Omega\sin\theta_o)]^{-2}$$
$$- \sec^2\ \frac{e}{a\sqrt{1 - e^2}}[\overline{X}(\cos\Omega\cos\theta_o - \sin\mu\ \sin\Omega\sin\theta_o)$$
$$- \overline{Y}\cos\mu\ \sin\theta_o - \overline{Z}(\sin\Omega\cos\theta_o + \sin\mu\ \cos\Omega\sin\theta_o)]$$
$$- \frac{k}{a^{3/2}}t\ (\cos\Omega\cos\theta_o - \sin\mu\ \sin\Omega\sin\theta_o)$$

$$a_{62} = \frac{1}{\sqrt{1 - e^2}}[-ae\cos\mu\ \sin\theta_o - \overline{X}\cos\Omega\cos\mu + \overline{Z}\sin\Omega\cos\mu\,]$$
$$[ae + \overline{X}(\cos\Omega\sin\theta_o + \sin\mu\ \sin\Omega\cos\theta_o) + Y\cos\mu\ \cos\theta_o$$
$$+ Z(\sin\mu\ \cos\Omega\cos\in_o \sin\Omega\sin\theta_o]^{-2}$$
$$+ \sec^2\ \frac{e}{a\sqrt{1 - e^2}}[\overline{X}(\cos\Omega\cos\theta_o - \sin\mu\ \sin\Omega\sin\theta_o)$$
$$- \overline{Y}\cos\mu\ \sin\theta_o - \overline{Z}(\sin\Omega\cos\theta_o + \sin\mu\ \cos\Omega\sin\theta_o)]$$
$$- \frac{k}{a^{3/2}}\ t\cos\mu\ \sin\theta_o$$

$$a_{63} = \frac{1}{\sqrt{1 - e^2}}\left[-ae(\sin\Omega \cos\theta_o + \sin\mu \cos\Omega \sin\theta_o) - \overline{X} \sin\mu \right.$$

$$\left. - \overline{Y} \cos\mu \sin\Omega\right]\left[ae + X(\cos\Omega \sin\theta_o + \sin\mu \sin\Omega \cos\theta_o) \right.$$

$$\left. + \overline{Y} \cos\mu \cos\theta_o + \overline{Z}(\sin\mu \cos\Omega \cos\theta_o - \sin\Omega \sin\theta_o)\right]^{-2}$$

$$+ \sec^2 \frac{e}{a\sqrt{1 - e^2}}\left[\overline{X}(\cos\Omega \cos\theta_o - \sin\mu \sin\Omega \sin\theta_o) \right.$$

$$\left. - \overline{Y} \cos\mu \sin\theta_o - \overline{Z}(\sin\Omega \cos\theta_o + \sin\mu \cos\Omega \sin\theta_o)\right]$$

$$- \frac{k}{a^{3/2}} t \ (\sin\Omega \cos\theta_o + \sin\mu \cos\Omega \sin\theta_o)$$

$$a_{64} = 0$$

$$a_{65} = 0$$

$$a_{66} = 0$$

As defined $X_1 = X$, $X_2 = Y$, $X_3 = Z$, $X_4 = \dot{X}$, $X_5 = \dot{Y}$, $X_6 = \dot{Z}$ and F_{10}, F_{20}, ... F_{60} are Equations (4-27), (4-28), ... (4-32) respectively, evaluated at the successive approximations to the state variables.

APPENDIX B

THE VARIATIONAL PROBLEM

1. 0 INTRODUCTION

The Euler-Lagrange equations for the variational docking problem, using minimum fuel consumption as the optimal criteria, are developed in Section 2. 0. The terminal conditions for the docking problem are defined in state variable notation in Section 3. 0. The Erdmann-Weirstrass corner conditions are given in Section 4. 0. The Weirstrass conditions for the existence of a minimum value are discussed in Section 5. 0, and the composition of extremal arcs are explored in some detail in Section 6. 0 to determine the form of the desired solution with the conditions governing it.

2. 0 EULER-LAGRANGE EQUATIONS

Using the nomenclature and coordinate system adopted above, the orientation of the thrust vector is defined by the following transformations:

$$\begin{pmatrix} x \\ y \\ z \end{pmatrix} = \begin{pmatrix} \cos X_p & - \sin x_p & 0 \\ \sin X_p & \cos X_p & 0 \\ 0 & 0 & 1 \end{pmatrix} \begin{pmatrix} x_1 \\ y_1 \\ z_1 \end{pmatrix}$$

$$\begin{pmatrix} x_1 \\ y_1 \\ z_1 \end{pmatrix} \begin{pmatrix} \cos X_r & 0 & -\sin X_r \\ 0 & 1 & 0 \\ \sin X_r & 0 & \cos X_r \end{pmatrix} \begin{pmatrix} x_2 \\ y_2 \\ z_2 \end{pmatrix}$$

$$\begin{pmatrix} x_2 \\ y_2 \\ z_2 \end{pmatrix} - \begin{pmatrix} 1 & 0 & 0 \\ 0 & \cos X_y & -\sin X_y \\ 0 & \sin X_y & \cos X_y \end{pmatrix} \begin{pmatrix} x_M \\ y_M \\ z_M \end{pmatrix}$$

where x, y, z are unit vectors in the plumbline coordinate system and x_M, y_M, z_M are the unit vectors along the body axis of the chaser. The thrust vector of the vehicle is defined to be along the y_M axis.

The problem is restricted to subarcs flown at and between maximum thrust and minimum thrust (maximum throttling). The thrust magnitude is defined by

$$T = \beta V_e \tag{2-1}$$

where V_e is the effective exhaust velocity and β is the propellant flow rate. To obtain the optimum thrust vector program, the roll angle (X_r) can be arbitrarily chosen as zero. Then the components of the thrust vector in the x, y, z system become

$$T_x = -(\sin X_p \cos X_y)\, \beta V_e \tag{2-2}$$

$$T_y = (\cos X_p \cos X_y)\, \beta V_e \tag{2-3}$$

$$T_z = (\sin X_y)\, \beta V_e \tag{2-4}$$

The three velocity components along the x, y, z axes are defined as U_4, U_5, and U_6 respectively, and the displacements as X_1, X_2, and X_3. Then for a central force field model, the first order set of differential equations governing the motion becomes,

$$\dot{g}_1 = U_4 + \frac{\beta V_e}{m} \sin X_p \cos X_y + \frac{g_o R_E^{\,2} X_1}{\left[X_1^{\,2} + X_2^{\,2} + X_3^{\,2}\right]^{3/2}} = 0 \tag{2-5}$$

$$\dot{g}_2 = \dot{U}_5 - \frac{\beta V_e}{m} \cos X_p \cos X_y + \frac{g_o R_E^{\,2} X_2}{\left[X_1^{\,2} + X_2^{\,2} + X_3^{\,2}\right]^{3/2}} = 0 \tag{2-6}$$

$$g_3 = U_6 - \frac{\beta V_e}{m} \sin X_y + \frac{g_o R_E^2 X_3}{\left[X_1^2 + X_2^2 + X_3^2\right]^{3/2}} = 0 \qquad (2\text{-}7)$$

$$g_4 = \dot{X}_1 - U_4 = 0 \qquad (2\text{-}8)$$

$$g_5 = \dot{X}_2 - U_5 = 0 \qquad (2\text{-}9)$$

$$g_6 = \dot{X}_3 - U_6 = 0 \qquad (2\text{-}10)$$

The vehicle's mass and the constraint on the mass flow are given by:

$$g_7 = \dot{m} + \beta = 0 \qquad (2\text{-}11)$$

$$g_8 = (\beta_u - \beta)(\beta - \beta_L) - \gamma^2 = 0 \qquad (2\text{-}12)$$

where

β_u and β_L = the upper and lower limits imposed on the allowable mass flow rate, respectively

γ = a real variable introduced to satisfy the constraint equation.

To minimize the fuel consumption, the integral

$$I = \int \beta dt \qquad (2\text{-}13)$$

must be minimized subject to the constraints given by equations (2-5) through (2-12).

To this end, the following function is defined:

$$G = \beta + \vec{g} \cdot \vec{\lambda} \qquad (2\text{-}14)$$

where

$\vec{g}$ = the eight-dimensional vector defined by Equations (2-5) through (2-12)

λ = the eight-dimensional vector to be defined by the Euler-Lagrange equation

$$\frac{\partial G}{\partial q} = \frac{d}{dt}\left(\frac{\partial G}{\partial \dot{q}}\right) \tag{2-15}$$

where

q = the variables U_1, U_2, U_3, X_1, X_2, X_3, m, β, X_p, X_y, and γ.

Evaluating Equation (2-15), the following set of differential equations results:

$$\dot{\lambda}_1 = \lambda_4 \tag{2-16}$$

$$\dot{\lambda}_2 = \lambda_5 \tag{2-17}$$

$$\dot{\lambda}_3 = \lambda_6 \tag{2-18}$$

$$\dot{\lambda}_4 = \frac{g_o R_E^2}{\left[X_1^2 + X_2^2 + X_3^2\right]^{3/2}}\left[\lambda_1\left(1 - \frac{3X_1^2}{X_1^2 + X_2^2 + X_3^2}\right) - \frac{3\lambda_2 X_2 X_1}{X_1^2 + X_2^2 + X_3^2} - \frac{3\lambda_3 X_3 X_1}{X_1^2 + X_2^2 + X_3^2}\right] \tag{2-19}$$

$$\dot{\lambda}_5 = \frac{g_o R_E^2}{\left[X_1^2 + X_2^2 + X_3^2\right]^{3/2}}\left[\lambda_2\left(1 - \frac{3X_2^2}{X_1^2 + X_2^2 + X_3^2}\right) - \frac{3\lambda_1 X_1 X_2}{X_1^2 + X_2^2 + X_3^2} - \frac{3\lambda_3 X_3 X_2}{X_1^2 + X_2^2 + X_3^2}\right] \tag{2-20}$$

$$\dot{\lambda}_6 = \frac{g_o R_E^2}{\left[X_1^2 + X_2^2 + X_3^2\right]^{3/2}} \left[\lambda_3\left(1 - \frac{3X_3^2}{X_1^2 + X_2^2 + X_3^2}\right) - \frac{3\lambda_1 X_1 X_3}{X_1^2 + X_2^2 + X_3^2} - \frac{3\lambda_2 X_2 X_3}{X_1^2 + X_2^2 + X_3^2}\right] \tag{2-21}$$

$$\dot{\lambda}_7 = -\lambda_1 \frac{\beta V_e}{m^2} \sin X_p \cos X_y + \lambda_2 \frac{\beta V_e}{m^2} \cos X_p \cos X_y + \lambda_3 \frac{\beta V_e}{m^2} \sin X_y \tag{2-22}$$

$$0 = \lambda_1 \frac{V_e}{m} \sin X_p \cos X_y - \lambda_2 \frac{V_e}{m} \cos X_p \cos X_y - \lambda_3 \frac{V_e}{m} \sin X_y + \lambda_7 + \lambda_8(-2\beta + \beta + \beta_L) + 1.0 \tag{2-23}$$

$$0 = \frac{\beta V_e}{m} \lambda_1 \cos X_p \cos X_y + \frac{\beta V_e}{m} \lambda_2 \sin X_p \cos X_y \tag{2-24}$$

$$0 = -\frac{\beta V_e}{m} \lambda_1 \sin X_p \sin X_y + \frac{\beta V_e}{m} \lambda_2 \cos X_p \sin X_y - \frac{\beta V_e}{m} \lambda_3 \cos X_y \tag{2-25}$$

$$0 = 2\gamma\lambda_8 \tag{2-26}$$

From Equations (2-24) and (2-25), the thrust direction is given by

$$\tan X_p = -\lambda_1/\lambda_2 \tag{2-24a}$$

$$\tan X_y = \frac{\lambda_3}{\sqrt{\lambda_1^2 + \lambda_2^2}} \tag{2-25a}$$

Equations (2-12) and (2-26) express the familiar condition that for subarcs flown at either $\beta = \beta_u$ or $\beta = \beta_L$, $\lambda_8 = 0$.

For this case, Equation (2-23) reduces to

$$\lambda_1 \frac{V_e}{m} \sin X_p \cos X_y - \lambda_2 \frac{V_e}{m} \cos X_p \cos X_y - \lambda_3 \frac{V_e}{m} \sin X_y + \lambda_7 + 1.0 = 0 \qquad (2\text{-}23a)$$

This equation when using Equations (2-24a) and (2-25a) can also be written

$$\lambda_7 = \frac{V_e}{m} \sqrt{\lambda_1^2 + \lambda_2^2 + \lambda_3^2} - 1.0 \qquad (2\text{-}23b)$$

Thus the necessary conditions for an optimum solution are summarized by the following equations:

$$\ddot{\overline{X}} = \frac{V_e \dot{m}_F}{m_R} \left[A_X\right]^T + \ddot{\overline{X}}_g$$

where

X = the three-dimensional vector with components X1, X2, and X3

V_e = the effective exhaust velocity

m_R = instantaneous mass

$\dot{m}_F$ = mass flow rate

$$\left[A_X\right]^T = \begin{bmatrix} -\sin X_p \cos X_y \\ \cos X_p \cos X_y \\ \sin X_y \end{bmatrix}$$

$$X_g = \frac{GM}{r^3} \overline{X}$$

$$r = \sqrt{\overline{X} \cdot \overline{X}}$$

The mass flow rate is given by

$$\dot{m}_F + \dot{m}_R = 0$$

The Euler-Lagrange equations are given by

$$\dot{\lambda}_i = -\frac{GM}{r^3}\left[\lambda_i - 3(\lambda_1 X_1 + \lambda_2 X_2 + \lambda_3 X_3)\frac{X_i}{r^2}\right]$$

where

$$i = 1, 2, 3$$

$$\dot{\lambda}_7 = \frac{V_e \dot{m}_F}{m_F^2}\left[\overline{\lambda}\right]^T \begin{bmatrix} -\sin X_p \cos X_y \\ \cos X_p \cos X_y \\ \sin X_y \end{bmatrix}$$

The thrust direction is given by

$$\tan X_p = \frac{\lambda_1}{\lambda_2}$$

$$\tan X_y = \frac{\lambda_3}{\sqrt{\lambda_1^2 + \lambda_2^2}}$$

The switching condition is given by

$$\Gamma = \frac{V_e}{m_R}\left[\overline{\lambda}\right]^T \begin{bmatrix} -\sin X_p \cos X_y & \\ \cos X_p \cos X_y & -\lambda_7 \\ \sin X_y & \end{bmatrix}$$

where

$$\dot{m}_F = (\dot{m}_F)_{MAX} \text{ when } \Gamma > 0$$

and

$$\dot{m}_F = (\dot{m}_F)_{MIN} \text{ when } \Gamma < 0$$

The boundary conditions are given at t = 0:

$$(\bar{X})_o = A$$

$$(\dot{\bar{X}})_o = B$$

$$(m_R)_o = C$$

at $t = t_f$

$$(\dot{X})_f = D$$

$$(\dot{\bar{X}})_f = E$$

$$(\lambda_7)_f = 1.0$$

It is noted that, in this general formulation, it is assumed that in the optimum solution variable, thrust sub-arcs exist. If examination of additional conditions indicates a restricted form of the optimum solution, the number of variables and equations will be reduced appropriately.

3.0 DEVELOPMENT OF BOUNDARY CONDITIONS

The terminal conditions for the docking problem are based upon the equations of Appendix A. They are written here in state variable notation, where the subscript "f" denotes the terminal value of a state variable.

$$\psi_1 = (U_4)_f^2 + (U_5)_f^2 + (U_6)_f^2 - \frac{2g_o R_E^2}{\sqrt{(X_1)_f^2 + (X_2)_f^2 = (X_3)_f^2}} + \frac{g_o R_E^2}{a} = 0 \tag{3-1}$$

$$\psi_2 = (X_2)_f(U_6)_f - (X_3)_f(U_5)_f - R_E\sqrt{ag_o}\sqrt{1 - e^2}\cos\mu \sin\Omega = 0 \tag{3-2}$$

$$\psi_2 = (X_3)_f(U_4)_f - (X_1)_f(U_6)_f + R_E\sqrt{ag_o}\sqrt{1 - e^2}\sin\mu = 0 \quad (3\text{-}3)$$

$$\psi_4 = (X_1)_f(U_5)_f - (X_2)_f(U_4)_f - R_E\sqrt{ag_o}\sqrt{1 - e^2}\cos\mu\cos\Omega = 0 \quad (3\text{-}4)$$

$$\psi_5 = \Big[(X_1)_f(\cos\Omega\cos\theta_o + \sin\mu\sin\Omega\sin\theta_o) + (X_2)_f\cos\mu\sin\theta_o + (X_3)_f(\sin\mu\cos\Omega\sin\theta_o - \sin\Omega\cos\theta_o)\Big]^2 + \frac{1}{(1 - e^2)}\Big[(X_1)_f(\sin\mu\sin\Omega\cos\theta_o - \cos\Omega\sin\theta_o) + (X_2)_f\cos\mu\cos\theta_o + (X_3)_f(\sin\Omega\sin\theta_o + \sin\mu\cos\Omega\cos\theta_o)\Big]^2 - a^2 = 0 \quad (3\text{-}5)$$

$$\psi_6 = \tan^{-1}\frac{1}{\sqrt{1 - e^2}}$$

$$\frac{(X_1)_f(\sin\mu\sin\Omega\cos\theta_o - \cos\Omega\sin\theta_o) - (X_2)_f\cos\mu\cos\theta_o + (X_3)_f(\sin\mu\cos\Omega\cos\theta_o + \sin\Omega\sin\theta_o)}{ae + (X_1)_f(\cos\Omega\cos\theta_o + \sin\mu\sin\Omega\sin\theta_o) + (X_2)_f\cos\mu\sin\theta_o + (X_3)_f(\sin\mu\cos\Omega\sin\theta_o - \sin\Omega\cos\theta_o)}$$

$$-\frac{e}{a\sqrt{1 - e^2}}(X_1)_f(\sin\mu\sin\Omega\cos\theta_o - \cos\Omega\sin\theta_o) + (X_2)_f\cos\mu\cos\theta_o + (X_3)_f(\sin\Omega\sin\theta_o + \sin\mu\cos\Omega\cos\theta_o) - \sqrt{\frac{R_E^2 g_o}{a^3}}(t_f - t_p) = 0$$

At the initial point, the conditions can be stated formally as:

$$\psi_7 = (X_1)_o - K_1 = 0 \quad (3\text{-}7)$$

$$\psi_8 = (X_2)_o - K_2 = 0 \quad (3\text{-}8)$$

$$\psi_9 = (X_3)_o - K_3 = 0 \quad (3\text{-}9)$$

$$\psi_{10} = (U_4)_o - K_4 = 0 \quad (3\text{-}10)$$

$$\psi_{11} = (U_5)_o - K_5 = 0$$

$$\psi_{12} = (U_6)_o - K_6 = 0$$

$$\psi_{13} = (m)_o - K_7 = 0$$

where t_o is chosen for convenience as zero.

Based on the theory of calculus of variations, the following set of boundary conditions have to be satisfied at the end-points for the problem of Lagrange with variable end-points.

$$-f]_o + \sum_{i=1}^{m} \left[q_i \frac{\partial f}{\partial q_i} + \sum_{j=1}^{m} \lambda_j \frac{\partial g_j}{\partial q_i} \right]_o + \sum_{\mu=1}^{p} \epsilon_\mu \frac{\partial \psi_\mu}{\partial t_o} = 0 \qquad (3\text{-}14)$$

$$f]_f - \sum_{i=1}^{m} \left[q_i \frac{\partial f}{\partial q_i} + \sum_{j=1}^{m} \lambda_j \frac{\partial g_j}{\partial q_i} \right]_f + \sum_{\mu=1}^{p} \epsilon_\mu \frac{\partial \psi_\mu}{\partial t_f} = 0 \qquad (3\text{-}15)$$

$$-\frac{\partial f}{\partial q_i}\Big]_o - \sum_{j=1}^{m} \lambda_j \frac{\partial g_i}{\partial q_i}\Big]_o + \sum_{\mu=1}^{p} \epsilon_\mu \frac{\partial \psi_\mu}{\partial q_{i(o)}} = 0 \qquad (3\text{-}16)$$

$$\frac{\partial f}{\partial q_i}\Big]_f + \sum_{j=1}^{m} \lambda_j \frac{\partial g_i}{\partial q_i}\Big]_f + \sum_{\mu=1}^{p} \epsilon_\mu \frac{\partial \psi_\mu}{\partial q_{i(f)}} = 0 \qquad (3\text{-}17)$$

where the generalized variable q_i represents the variables X_1, X_2, X_3, ..., and g_j the equations g_1, g_2, ..., g_8. The parameters ϵ_μ represent constants to be determined from the above set of equations, and the parameter f is the integrand of the integral to be minimized.

Evaluation of Equation (3-14) yields

$$\left[-\beta + \lambda_1 \dot{U}_4 + \lambda_2 \dot{U}_5 + \lambda_3 \dot{U}_6 + \lambda_4 \dot{X}_1 + \lambda_5 \dot{X}_2 + \lambda_6 \dot{X}_3 + \lambda_7 \dot{m} \right]_o = 0$$

Evaluation of Equation (3-15) yields

$$-\left[-\beta+\lambda_1\dot{U}_4+\lambda_2\dot{U}_5+\lambda_3\dot{U}_6+\lambda_4\dot{X}_1+\lambda_5\dot{X}_2+\lambda_6\dot{X}_3+\lambda_7\dot{m}\right]_f-\epsilon_6\sqrt{\frac{R_E^{\,2}g_o}{a^3}}=0 \tag{3-19}$$

Evaluation of Equation (3-16) yields

$$\begin{aligned}
-(\lambda_1)_o+\epsilon_{10} &= 0\\
-(\lambda_2)_o+\epsilon_{11} &= 0\\
-(\lambda_3)_o+\epsilon_{12} &= 0\\
-(\lambda_4)_o+\epsilon_{7} &= 0\\
-(\lambda_5)_o+\epsilon_{8} &= 0\\
-(\lambda_6)_o+\epsilon_{9} &= 0\\
-(\lambda_7)_o+\epsilon_{13} &= 0
\end{aligned} \tag{3-20}$$

Evaluation of Equation (3-17(yields

$$(\lambda_1)_f+2\epsilon_1(U_4)_f+\epsilon_3(X_3)_f-\epsilon_4(X_2)_f=0 \tag{3-21}$$

$$(\lambda_2)_f+2\epsilon_1(U_5)_f-\epsilon_2(X_3)_f+\epsilon_4(X_1)_f=0 \tag{3-22}$$

$$(\lambda_3)_f+2\epsilon_1(U_6)_f-\epsilon_2(X_2)_f-\epsilon_3(X_1)_f=0 \tag{3-23}$$

$$\begin{aligned}
&(\lambda_4)_f+\frac{2\epsilon_1 g_o R_E^{\,2}(X_1)_f}{\left[(X_1)_f^{\,2}+(X_2)_f^{\,2}+(X_3)_f^{\,2}\right]^{3/2}}-\epsilon_3(U_6)_f+\epsilon_4(U_5)_f\\
&+2\epsilon_5\left[(X_1)_f(\cos\Omega\cos\theta_o+\sin\mu\sin\Omega\sin\theta_o)\right.\\
&\left.+(X_2)_f\cos\mu\sin\theta_o+(X_3)_f(\sin\mu\cos\Omega\sin\theta_o-\sin\Omega\cos\theta_o)\right]\\
&(\cos\Omega\cos\theta_o+\sin\mu\sin\Omega\sin\theta_o)
\end{aligned} \tag{3-24}$$

$$+\frac{2\epsilon_5}{(1-e^2)}\left[(X_1)_f(\sin\mu\ \sin\Omega\cos\theta_o-\cos\Omega\sin\theta_o)\right.$$

$$\left.+(X_2)_f\cos\mu\ \cos\theta_o+(X_3)_f(\sin\Omega\sin\theta_o+\sin\mu\ \cos\Omega\cos\theta_o)\right]$$

$$(\sin\mu\ \sin\Omega\cos\theta_o-\cos\Omega\sin\theta_o) \qquad (2\text{-}24)$$

$$+\frac{\frac{6}{\sqrt{1-e^2}}D(\sin\mu\ \sin\Omega\cos\theta_o-\cos\Omega\sin\theta_o)-N(\cos\Omega\cos\theta_o+\sin\mu\ \sin\Omega\sin\theta_o)}{D^2+\frac{1}{1-e^2}N^2}$$

$$-\frac{\epsilon_6 e}{a\sqrt{1-e^2}}(\sin\mu\ \sin\Omega\cos\theta_o-\cos\Omega\sin\theta_o)=0$$

where

$$N=(X_1)_f(\sin\mu\ \sin\Omega\cos\theta_o-\cos\Omega\sin\theta_o)-(X_2)_f\cos\mu\ \cos\theta_o$$
$$+(X_3)_f(\sin\mu\ \cos\Omega\cos\theta_o+\sin\Omega\sin\theta_o)$$

$$D=ae+(X_1)_f(\cos\Omega\cos\theta_o+\sin\mu\ \sin\Omega\sin\theta_o)+(X_2)_f\cos\mu\ \sin\theta_o$$
$$+(\dot{X}_3)_f(\sin\mu\ \cos\Omega\sin\theta_o-\sin\Omega\cos\theta_o)$$

$$(\lambda_5)_f+\frac{2\epsilon_1 g_o R_E^2(X_2)_f}{\left[(X_1)_f^2+(X_2)_f^2+(X_3)_f^2\right]^{3/2}}+\epsilon_2(U_6)_f-\epsilon_4(U_4)_f$$
$$+2\epsilon_5\left[(X_1)_f(\cos\Omega\cos\theta_o+\sin\mu\ \sin\Omega\sin\theta_o)+(X_2)_f\cos\mu\ \sin\theta_o\right.$$
$$\left.+(X_3)_f(\sin\mu\ \cos\Omega\sin\theta_o-\sin\Omega\cos\theta_o)\right]\cos\mu\ \sin\theta_o$$
$$+\frac{2\epsilon_5}{(1-e^2)}\left[(X_1)_f(\sin\mu\ \sin\Omega\cos\theta_o-\cos\Omega\sin\theta_o)+(X_2)_f\text{cow}\mu\ \cos\theta_o\right.$$

$$+ (X_3)_f (\sin\Omega \sin\theta_o + \sin\mu \cos\Omega \cos\theta_o) \cos\mu \cos\theta_o$$

$$+ \frac{\frac{\epsilon_6}{\sqrt{1-e^2}} - D\cos\mu\cos\theta_o - N\cos\mu\sin\theta_o}{D^2 + \frac{1}{1-e^2}N^2}$$

$$- \frac{\epsilon_6 e}{a\sqrt{1-e^2}} (\sin\mu \sin\Omega \cos\theta_o - \cos\Omega \sin\theta_o) = 0 \qquad (3\text{-}25)$$

with the parameters D and N as defined above.

$$(\lambda_6)_f + \frac{2\epsilon_1 g_o R_E^2 (X_3)_f}{\left[(X_1)_f^2 + (X_2)_f^2 + (X_3)_f^2\right]^{3/2}} - \epsilon_2 (U_5)_f + \epsilon_3 (U_4)_f$$

$$+ 2\epsilon_5 (X_1)_f (\cos\Omega \cos\theta_o + \sin\mu \sin\Omega \sin\theta_o) + (X_2)_f \cos\mu \sin\theta_o$$

$$+ (X_3)_f (\sin\mu \cos\Omega \sin\theta_o - \sin\Omega \cos\theta_o)(\sin\mu \cos\Omega \sin\theta_o - \sin\Omega \cos\theta_o)$$

$$+ \frac{2\epsilon_5}{(1-e^2)}\Big[(X_1)_f (\sin\mu \sin\Omega \cos\theta_o - \cos\Omega \sin\theta_o) + (X_2)_f \cos\mu \cos\theta_o$$

$$+ (X_3)_f (\sin\Omega \sin\theta_o + \sin\mu \cos\Omega \cos\theta_o)(\sin\Omega \sin\theta_o + \sin\mu \cos\Omega \cos\theta_o)\Big]$$

$$+ \frac{\frac{\epsilon_6}{\sqrt{1-e^2}} D(\sin\mu \cos\Omega \cos\theta_o + \sin\Omega \sin\theta_o) - N(\sin\mu \cos\Omega \sin\theta_o - \sin\Omega \cos\theta_o)}{D^2 + \frac{1}{1-e^2}N^2}$$

$$- \frac{\epsilon_6 e}{a\sqrt{1-e^2}} (\sin\Omega \sin\theta_o + \sin\mu \cos\Omega \cos\theta_o) = 0 \qquad (3\text{-}26)$$

$$(\lambda_7)_f = 0 \tag{3-27}$$

The six Equations (3-21) through (3-26) specify the constants $\epsilon_1, \epsilon_2, \ldots\ldots, \epsilon_6$. Since these constants are now known, equations (3-21) through (3-26) do not furnish any additional information. To determine the boundary conditions for the 14 first order differential equations (2-5) through (2-11) and (2-16) through (2-22), the boundary conditions can be most easily specified by equations (3-7) through (3-13), (3-1) through (3-6), (3-18), and (3-27). It is noted that a total of 15 boundary conditions are required, since the final time (t_f) is not specified.

4.0 CORNER CONDITIONS

It is noted from Equations (2-5) through (2-12) that $\ddot{U}_4$, $\ddot{U}_5$, $\ddot{U}_6$, $\dot{X}_y$, X_p, and β do not appear in the differential equations. Thus U_4, U_5, U_6, X_y, X_p, and β are required to be only piecewise continuous in the interval $t_o \leq t \leq t_f$; i.e., the extremal arc may have corners. At such corners, the Erdmann-Weierstrass corner conditions must be satisfied. For the problem considered, this implies that at such corners

$$\lambda_j(+) = \lambda_j(-); \; j = 1, 2, \ldots\ldots, 7 \tag{4-1}$$

Equation (4-1) is a statement of that fact that the multipliers $\lambda_1, \lambda_2, \ldots\ldots, \lambda_7$ must remain continuous over the interval $t_o \leq t \leq t_f$.

5.0 WEIERSTRASS CONDITIONS

To explore the nature of the optimum solution in some more detail, one of the necessary conditions for the existance of a minimum value of

$$I = \int_{t_o}^{t_f} \beta dt,$$

is now considered. This is the Weierstrass condition, which requires that the function

$$E = G(q_i^*, \dot{q}_i) - G(q_i, \dot{q}_i) - \sum_{i=1}^{11} (q_i^* - q_i) \frac{\partial G}{\partial \dot{q}_i} \tag{5-1}$$

where G is defined by

$$G = \beta + \bar{g} \cdot \bar{\lambda}, \tag{5-2}$$

satisfy the inequality

$$E \geq 0 \tag{5-3}$$

The functions q_i^* denote functions q_i subjected to finite admissable variations. It is evident that functions whose derivatives appear in Equations (2-5) through (2-12) cannot be subjected to variations. This implies that

$$U_4^* = U_4,\ U_5^* = U_5,\ U_6^* = U_6,\ X_1^* = X_1,\ X_2^* = X_2,\ X_3^* = X_3, \text{ and } M^* = m.$$

Evaluating inequality (5-3) yields

$$\beta\Gamma - \beta^*\Gamma^* \geq 0 \tag{5-4}$$

where

$$\Gamma = \frac{V_e}{m}(-\lambda_1 \cos X_y \sin X_p + \lambda_2 \cos X_p \cos X_y + \lambda_3 \sin X_y) - (1 + \lambda_7) \tag{5-5}$$

$$\Gamma^* = \frac{V_e}{m}(-\lambda_1 \cos X_y^* \sin X_p^* + \lambda_2 \cos X_p^* \cos X_y^* + \lambda_3 \sin X_y^*) - (1 + \lambda_7) \tag{5-6}$$

Since inequality (5-4) must hold for all admissable variations, we consider first

$$\beta = \beta^*$$

$$X_y \neq X_y^*,\ X_p \neq X_y^*$$

Inequality (5-4) becomes

$$-\lambda_1 \cos X_y \sin X_p + \lambda_2 \cos X_p \cos X_y + \lambda_3 \sin X_y - \left[-\lambda_1 \cos X_y^* \sin X_p^* + \lambda_2 \cos X_p^* \cos X_y^* + \lambda_3 \sin X_y^*\right] \geq 0 \tag{5-7}$$

Now consider

$$\beta \neq \beta^*$$

$$X_y = X_y^*,\ X_p = X_p^*$$

Inequality (5-4) becomes

$$(\beta - \beta^*)\Gamma \geq 0 \tag{5-8}$$

In equality (5-8) consider

$$\beta = \beta_u$$

Then

$$(\beta_u - \beta^*)\Gamma \geq 0 \tag{5-9}$$

For $\beta = \beta_L$, inequality (5-8) becomes

$$(\beta_L - \beta^*)\Gamma \geq 0 \tag{5-10}$$

Considering the results to be drawn from the Weierstrass condition, note first that the thrust vector orientation should be chosen such that for all admissable variations in X_p and X_y, the function

$$-\lambda_1 \cos X_y \sin X_p + \lambda_2 \cos X_p \cos X_y + \lambda_3 \sin X_y$$

is maximized at all times (inequality (5-7)).

Since by Equation (2-12)

$$\begin{aligned} \beta^* &> \beta_L \\ \beta^* &< \beta_u \end{aligned} \tag{5-11}$$

It follows from Equations (5-9) and (5-10) that

$$\Gamma \geq 0 \text{ when } \beta = \beta_u$$
$$\Gamma \leq 0 \text{ when } \beta = \beta_L \tag{5-12}$$

From Equation (2-23) also note that

$$\Gamma = \lambda_8(-2\beta + \beta_u + \beta_L) \tag{5-13}$$

Applying conditions (5-12) to Equation (5-13), the following conditions are obtained:

$$\lambda_8[\beta_L - \beta_u] \geq 0$$
$$\lambda_8[\beta_u - \beta_L] \leq 0 \tag{5-14}$$

Since by definition $\beta_u > \beta_L$, inequalities (5-14) imply that for the two cases of β considered

$$\lambda_8 \leq 0 \tag{5-15}$$

By application of the Weierstrass condition, inequality (5-15) can be shown to hold for all values of β.

6.0 NATURE OF OPTIMAL ARCS

The composition of the extremal arcs will be explored in some detail to determine the form of the desired solution with the conditions governing it.

From Equation (2-26) the following must hold

$$\lambda_8 = 0, \gamma \neq 0; \beta_L < \beta < \beta_u$$

$$\lambda_8 \neq 0, \gamma = 0; \beta = \beta_L \text{ or } \beta = \beta_u$$

or

$$\lambda_8 = 0, \gamma = 0; \beta = \beta_L \text{ or } \beta = \beta_u$$

Considered first is the existence of a solution when $\lambda_8 = 0$. When $\lambda_8 = 0$, Equation (2-23a) applies; i.e., $\Gamma = 0$. For Γ to remain equal to zero $\dot{\Gamma}$ must equal zero.

Differentiation of Γ yields

$$\dot{\Gamma} = -\frac{V_e}{m}\frac{\lambda_1\lambda_4 + \lambda_2\lambda_5 + \lambda_3\lambda_6}{\sqrt{\lambda_1^2 + \lambda_2^2 + \lambda_3^2}} \tag{6-1}$$

This can also be written

$$\dot{\Gamma} = \frac{V_e}{m}(-\lambda_4 \sin X_p \cos X_y + \lambda_5 \cos X_p \cos X_y + \lambda_6 \sin X_y) \tag{6-2}$$

If $\dot{\Gamma}$ is zero from Equation (6-1) or (6-2),

$$-\lambda_4 \sin X_p + \lambda_5 \cos X_p + \lambda_6 \tan X_y = 0$$

or

$$\frac{\lambda_4\lambda_1}{\sqrt{\lambda_1^2 + \lambda_2^2}} + \frac{\lambda_5\lambda_2}{\sqrt{\lambda_1^2 + \lambda_2^2}} + \frac{\lambda_6\lambda_3}{\sqrt{\lambda_1^2 + \lambda_2^2}} = 0$$

In general, this would be satisfied if

$$\lambda_4 = \lambda_5 = \lambda_6 = 0 \text{ for } \lambda_1 \neq 0,\ \lambda_2 \neq 0,\ \lambda_3 \neq 0$$

Referring to Equations (2-16), (2-17), and (2-18), this implies that

$$\lambda_1 = \text{const.}$$

$$\lambda_2 = \text{const.}$$

$$\lambda_3 = \text{const.}$$

But if $\lambda_4 = \lambda_5 = \lambda_6 = 0$, it follows that $\dot{\lambda}_4 = \dot{\lambda}_5 = \dot{\lambda}_6 = 0$. Using Equations (2-19), (2-20), and (2-21), this implies that $\lambda_1 = \lambda_2 = \lambda_3 = 0$. But under these conditions, no solution exists. Thus, in the optimum solution only subarcs of minimum or maximum thrust can arise; i.e.,

$$\beta = \beta_L \text{ or}$$

$$\beta = \beta_u \text{ only.}$$

As was shown by application of the Weierstrass condition

$$\Gamma \leq 0 \text{ when } \beta = \beta_L$$

$$\Gamma \geq 0 \text{ when } \beta = \beta_u,$$

then since no intermediate thrust levels can exist, the switching from

$$\beta = \beta_L \text{ to } \beta = \beta_u$$

must occur when

$$\Gamma = 0 \tag{6-3}$$

From Equations (2-24a) and (2-25a), the optimum thrust direction is given by

$$\tan X_p = -\lambda_1/\lambda_2 \tag{6-4}$$

$$\tan X_y = \frac{\lambda_3}{\sqrt{\lambda_1^2 + \lambda_2^2}} \tag{6-5}$$

The Edmann-Weierstrass corner condition insures that the multipliers $\lambda_1, \lambda_2, \ldots\ldots, \lambda_8$ remain continuous at all times in the interval $t_o \leq t \leq t_f$. This implies that tan X_p and tan X_y remain continuous throughout the solution.

However, Equations (604) and (6-5) admit jumps in X_p and X_y of magnitude π. This ambiguity is resolved by one of the results of applying the Weierstrass condition which requires that the expression

$$-\lambda_1 \cos X_y \sin X_p + \lambda_2 \cos X_p \cos X_y + \lambda_3 \sin X_y$$

be maximized at all times.

This then determines the principal values of X_p and X_y uniquely.

Thus it is shown that only subarcs flown at either minimum or maximum thrust exist for the optimum solution. The sign of the parameter Γ determines which value of ($\beta = \beta_L$) or ($\beta = \beta_u$) applies.

APPENDIX C

SIMPLIFIED FORMULATION FOR FEASIBILITY DETERMINATION

1.0 INTRODUCTION

The feasibility of the complete three dimensional formulation (discussed in Appendices A and B) was checked by simplifying the formulation, implementing the equations on a digital computer, and computing trial solutions. The simplified formulation is defined in Section 2.0, and a two impulse (idealized) solution is given in Section 3.0 to allow initial guesses for the Lagrange multipliers. Section 4.0 and 5.0 give some coordinate transformations which ease computational difficulties.

2.0 SIMPLIFIED MODEL

2.1 GENERAL

A two-dimensional model derived from the three-dimensional model defined above, is described in this section. It is this model which was used as a basis for a computer study to obtain optimum trajectories.

The target is assumed to be in a circular orbit, and the chaser is in a coplanar orbit, nearly at the same altitude and trailing by a small central angle. It is desired to obtain a fuel optimum rendezvous trajectory for a fixed time to rendezvous. The geometry of this trajectory is shown in Figure C-1. The radial distance of the target is r_T; the initial radial distance of the chaser is r_L. The central angle between chaser and target at commencement of rendezvous (launch) is ϕ_0. The anglar distance of the chaser vehicle trajectory is ψ.

In order to obtain the necessary fuel optimum trajectories, initial conditions must be found for the Euler Lagrange equations given below

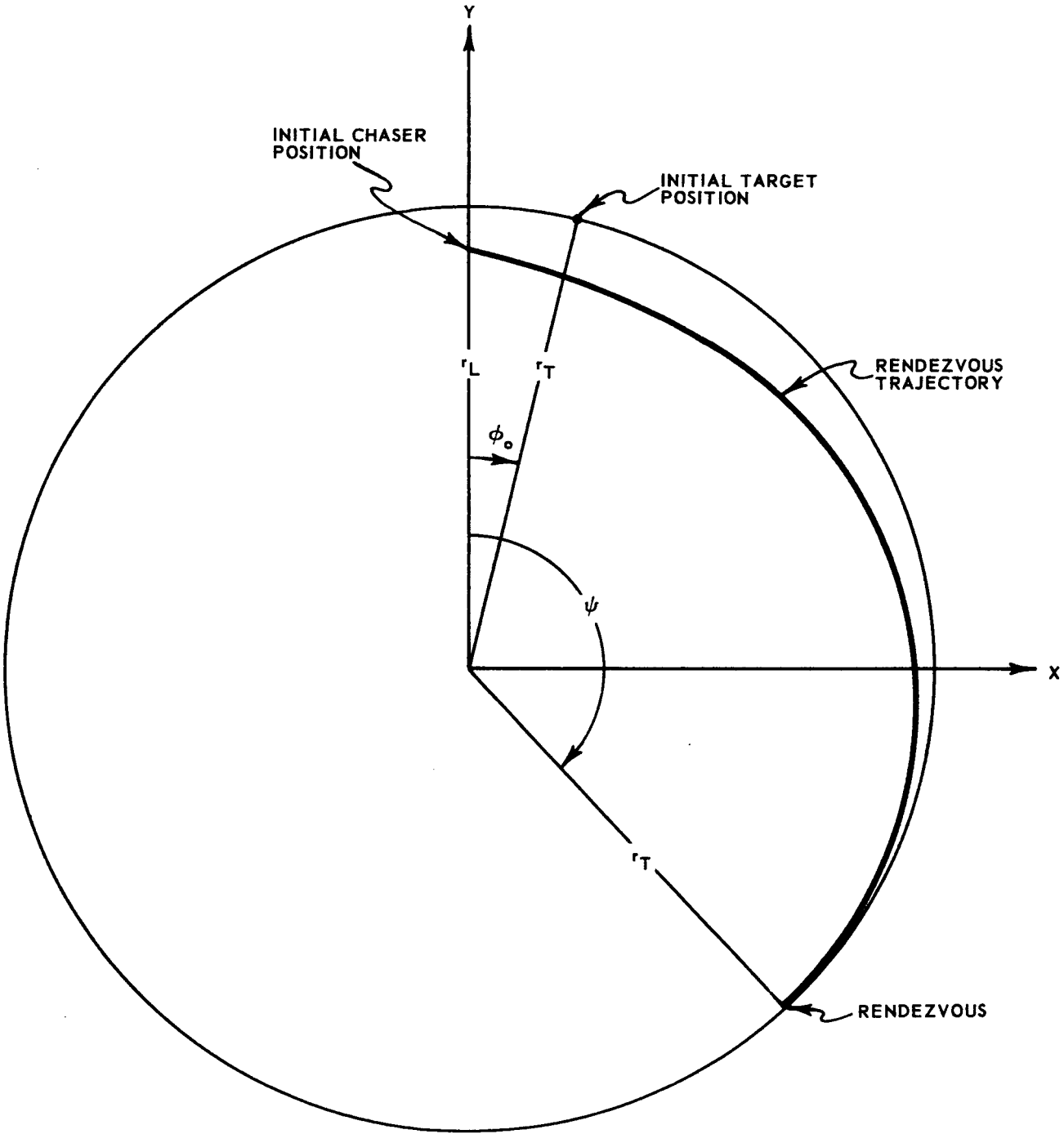

Figure C-1 Two-Dimensional Rendezvous Geometry

2.2 TWO-DIMENSIONAL CHASER EQUATIONS OF MOTION

These equations are derived from Appendix B, Equation (2-5) through (2-10):

$$\dot{X}_1 - U_4 = 0 \tag{2-1}$$

$$\dot{X}_2 - U_5 = 0 \tag{2-2}$$

$$\dot{U}_4 + \frac{\beta V_e}{m} \sin X_p + \frac{g_0 R_E^2 X_1}{\left[X_1^2 + X_2^2\right]^{3/2}} = 0 \tag{2-3}$$

$$\dot{U}_5 - \frac{\beta V_e}{m} \cos X_p + \frac{g_0 R_E^2 X_2}{\left[X_1^2 + X_2^2\right]^{3/2}} = 0 \tag{2-4}$$

$$\dot{m} + \beta = 0 \tag{2-5}$$

2.3 EULER LAGRANGE EQUATIONS

These equations are derived from Appendix B, Equation (2-16) through (2-26):

$$\dot{\lambda}_1 = -\lambda_3 \tag{2-6}$$

$$\dot{\lambda}_2 = -\lambda_4 \tag{2-7}$$

$$\dot{\lambda}_3 = \frac{g_0 R_E^2}{\left[X_1^2 + X_2^2\right]^{3/2}} \quad \lambda_1 \left[1 - \left(\frac{3 X_1^2}{X_1^2 + X_2^2}\right) - \frac{3\lambda_2 X_1 X_2}{X_1^2 + X_2^2}\right] \tag{2-8}$$

$$\dot{\lambda}_4 = \frac{g_0 R_E^2}{\left[X_1^2 + X_2^2\right]^{3/2}} \left[\lambda_2 \left(1 - \frac{3 X_2^2}{X_1^2 + X_2^2}\right) - \frac{3\lambda_1 X_1 X_2}{X_1^2 + X_2^2}\right] \quad (2\text{-}9)$$

$$\dot{\lambda}_5 = \frac{\beta V_e}{m^2} \left[-\lambda_1 \sin X_p + \lambda_2 \cos X_p\right] \quad (2\text{-}10)$$

$$\tan X_p = -\lambda_1 / \lambda_2 \quad (2\text{-}11)$$

$$\Gamma = \frac{V_e}{m} \left[-\lambda_1 \sin X_p + \lambda_2 \cos X_p\right] - \lambda_5 - 1 \quad (2\text{-}12)$$

$$\beta = \beta_U \text{ when } \Gamma > 0 \quad (2\text{-}13)$$

$$\beta = \beta_L \text{ when } \Gamma < 0$$

3.0 TWO IMPULSE SOLUTION

Since, for large thrust engines, the optimum trajectory will be close to a two-impulse transfer, the two impulse transfer case is now solved in order to obtain initial guesses for the Lagrange multipliers.

The polar equation of a transfer orbit is, in general, given by

$$r = \frac{p}{1 + e \cos v} \quad (3\text{-}1)$$

where

r is the radial distance

p is the latus rectum

e is the eccentricity, and

v is the true anomoly.

At launch $r = r_L$ and the corresponding true anomoly is v_L. If ψ is the central angle subtended between launch and rendezvous, then at rendezvous, $r = r_T$ and $v = v_L + \psi$. This is shown in Figure C-2. Hence, substituting launch and rendezvous conditions into Equation (3-1) and eliminating p yields:

$$e = \frac{r_L - r_T}{r_T \cos(v_L + \psi) - r_L \cos v_L} \tag{3-2}$$

where $r_L = r_T$.

The constant angular rate of the target is given by $\sqrt{k/r_T^3}$ where k is defined in Appendix B. Since the target moves through an angle $\psi - \phi_o$, the time to rendezvous is given by

$$\tau = \frac{r_T^{3/2}}{k^{1/2}} (\psi - \phi_o) \tag{3-3}$$

In general, the time of flight between two angular positions v_1 and v_2 in an eliptical orbit is given by

$$t = \frac{p^{3/2}}{k^{1/2}(1-e)^2} \left[-\frac{e \sin v}{1+e\cos v} + \frac{1}{\sqrt{1-e^2}} \tan^{-1} \frac{\sqrt{1-e^2}\sin v}{e+\cos v} \right]_{v_1}^{v_2} \tag{3-4}$$

Substituting $v_1 = v_L$, $v_2 = v_L + \psi$, $t = \tau$, and eliminating p by substituting $v = v_L + \psi$ and $r = r_T$ into Equation (3-1), yields, from Equation (3-4):

$$\psi - \phi_o = \frac{\left[1+e\cos(v_L+\psi)\right]^{3/2}}{(1-e^2)} \left[-\frac{e\sin v}{1+e\cos v} + \frac{1}{\sqrt{1-e^2}} \tan^{-1} \frac{\sqrt{1-e^2}\sin v}{e+\cos v} \right]_{v_L}^{v_L+\psi}$$

where e is defined by Equation (3-2). Equation (3-5) can now be solved for v_L, which then yields a value for e from Equation (3-2) and p from Equation (3-1). Thus, the transfer orbit is determined.

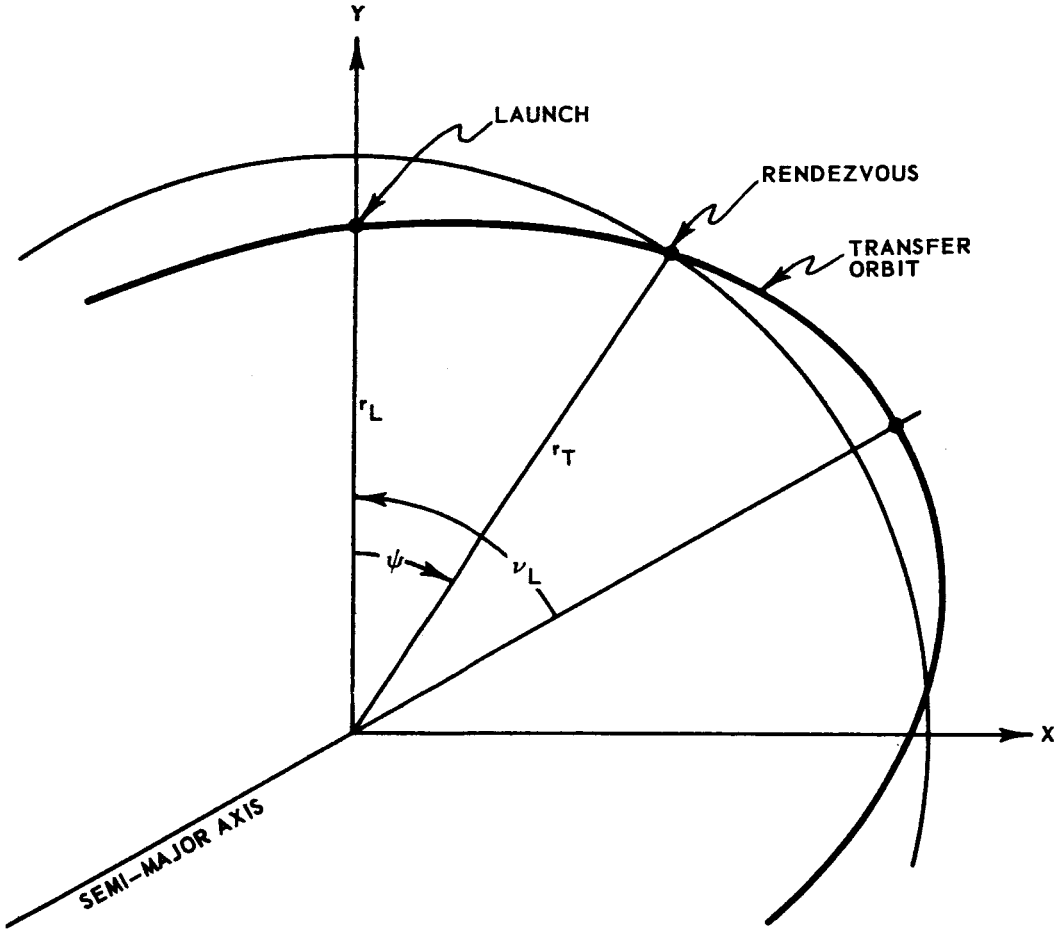

Figure C-2 Geometry of Rendezvous Trajectory, $r_L \neq r_T$

The solution fails if $r_L = r_T$ since $r_T \cos(v_L + \psi) = r_L \cos v_L$. For this case, $v_L = -\psi/2$ (or $\pi - \psi/2$). This is demonstrated in Figure C-3.

Substituting $v_2 = \psi/2$, $v_1 = -\psi/2$, and $t = \tau$ into Equation (3-4), and allowing $p/r_T = 1+e \cos \psi/2$ yields:

$$\psi - \phi_o = \frac{2(1+e\cos\psi/2)^{3/2}}{1-e^2}\left[\frac{e\sin\psi/2}{1+e\cos\psi/2} - \frac{1}{1-e^2}\tan^{-1}\frac{\sqrt{1-e^2}\sin\psi/2)}{e+\cos\psi/2}\right] \tag{3-6}$$

Equation (3-6) can be solved for e. This determines p, and thus the orbit is again determined.

The magnitude and direction of the impulsive velocity increments at launch and rendezvous can now be evaluated. If V_0 is the magnitude of the initial velocity vector, γ_o its direction with respect to the local horizontal, V_L and γ_L the velocity magnitude and direction after the first impulse, then the magnitude and direction of the first impulses given by, from Figure C-4.

$$\Delta V_L = \left[V_L^2 + V_0^2 - 2V_o V_L \cos(\gamma_L - \gamma_0)\right]^{1/2} \tag{3-7}$$

$$\beta_L = \tan^{-1}\frac{V_L \sin\gamma_L - V_0\cos\gamma_0}{V_L\cos\gamma_L - V_0\sin\gamma_0}$$

where

$$\gamma_L = \tan^{-1}\frac{e\sin v_L}{1+e\cos v_L} \tag{3-8}$$

$$V_L^2 = 2k\left[\frac{1}{r_L} - \frac{1}{2p(1-e^2)}\right]$$

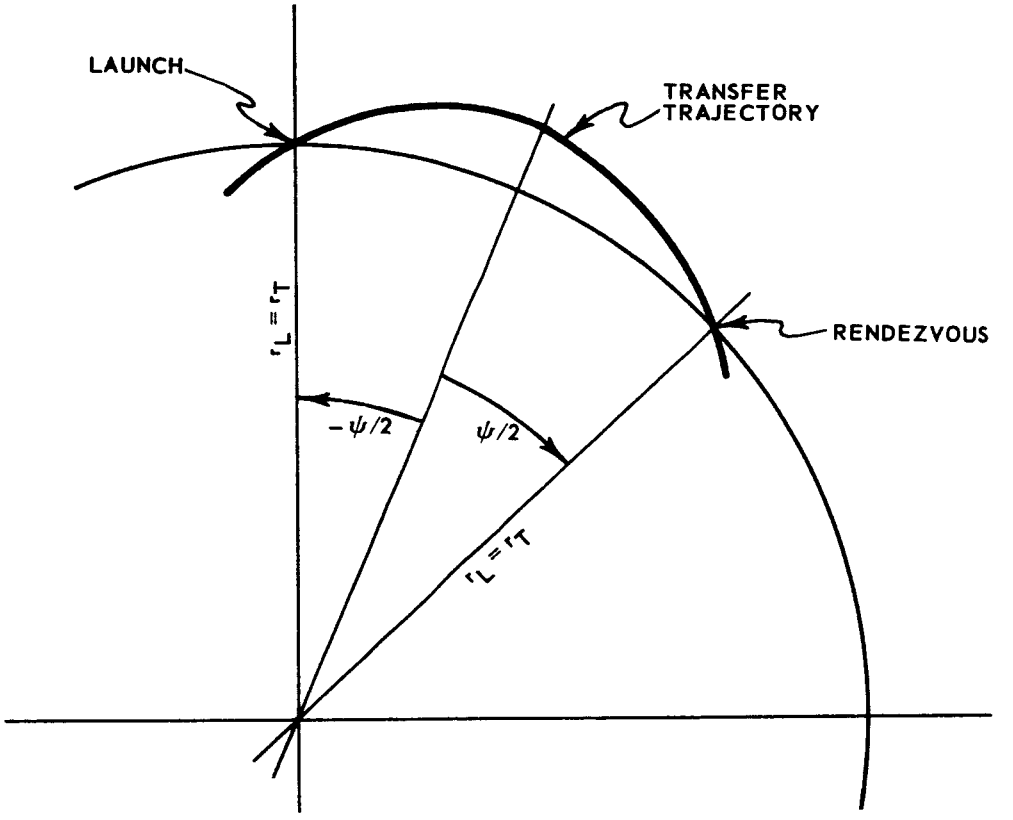

Figure C-3 Geometry of Rendezvous Trajectory, $r_L = r_T$

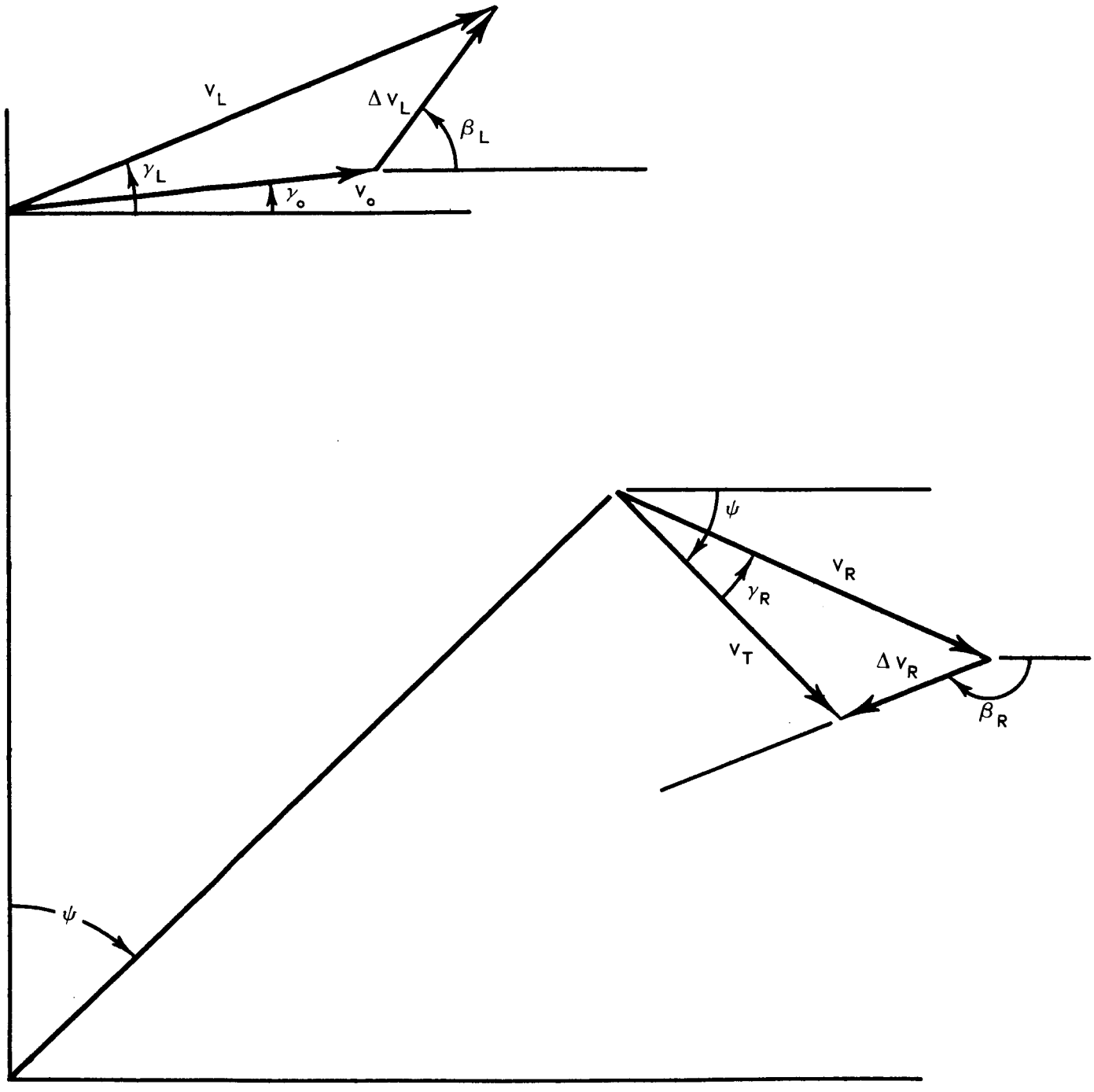

Figure C-4 Geometry of Velocity Increments

The magnitude and direction of the final impulse are defined by the following equations (see Figure C-4):

$$\Delta V_R = \left[V_R^2 + V_T^2 - 2V_R V_T \cos \gamma_R \right]^{1/2}$$

$$\beta_R = \tan^{-1} \frac{- \left[V_T \sin \psi - V_R \sin (\psi - \gamma_R) \right]}{V_T \cos \psi - V_R \cos (\psi - \gamma_R)} \qquad (3\text{-}9)$$

where

$$\gamma_R = \tan^{-1} \frac{e \sin (v_L + \psi)}{1 + e \cos (v_L + \psi)}$$

$$V_R^2 = 2k \left[\frac{1}{r_T} - \frac{1}{2p(1-e^2)} \right] \qquad (3\text{-}10)$$

$$V_T^2 = k/r_T$$

If it is assumed that the burning rate is constant, and that the thrust is constant, then the firing times can be approximated by

$$t_L = \frac{m_0}{\dot{m}} \left[1 - \exp (- \Delta V_L \dot{m} / T) \right]$$

$$t_R = \frac{m_1}{\dot{m}} \left[1 - \exp (- \Delta V_R \dot{m} / T) \right] \qquad (3\text{-}11)$$

where

t_L is the launch firing time

t_R is rendezvous firing time,

m_0 is the initial chaser mass, and

$m_1 = m_0 - \dot{m}\, t_L$.

Also, the final mass ratio is given by

$$\frac{m}{m_0} = \exp\left[-(\Delta V_L + \Delta V_R)\,\dot{m}/T\right] \tag{3-12}$$

A computer program was written to evaluate the various relevant quantities for a particular set of initial conditions: V_L, γ_L, r_L, ϕ_0, and r_T. The results shown in Figure C-5 demonstrate that the value of ψ over a very wide range has very little effect on ΔV. Similarly, Figure C-6 demonstrates the small effect of ψ on mass ratio. Conversely, very small variations in the magnitude and direction of the velocity increments have very large effects onthe rendezvous point. This implies that the initial values of the Lagrange multipliers are similarly sensitive in the calculus of variations model. This has been verified by computer runs.

4.0 COMPUTER CALCULUS OF VARIATIONS MODEL

The equations of Section 2 were transformed to polar form and are given below. The geometry is shown in Figure C-7.

$$\begin{aligned}
\ddot{r}\theta + 2\dot{r}\dot{\theta} &= -T/m \sin(\theta - \eta) \\
\ddot{r} - r\dot{\theta}^2 &= \frac{T}{m}\cos(\theta - \eta) - k/r^2 \\
\lambda\ddot{\eta} + 2\dot{\lambda}\dot{\eta} &= \frac{3k\lambda}{2r^3}\sin 2(\theta - \eta) \\
\ddot{\lambda} - \lambda\dot{\eta}^2 &= \frac{k\lambda}{2r^3}\left[1+3\cos 2(\theta - \eta)\right]
\end{aligned} \tag{4-1}$$

$$\dot{\lambda}_5 = \frac{T}{m^2}\lambda$$

$$\dot{\Gamma} = \frac{V_e}{m}\dot{\lambda}$$

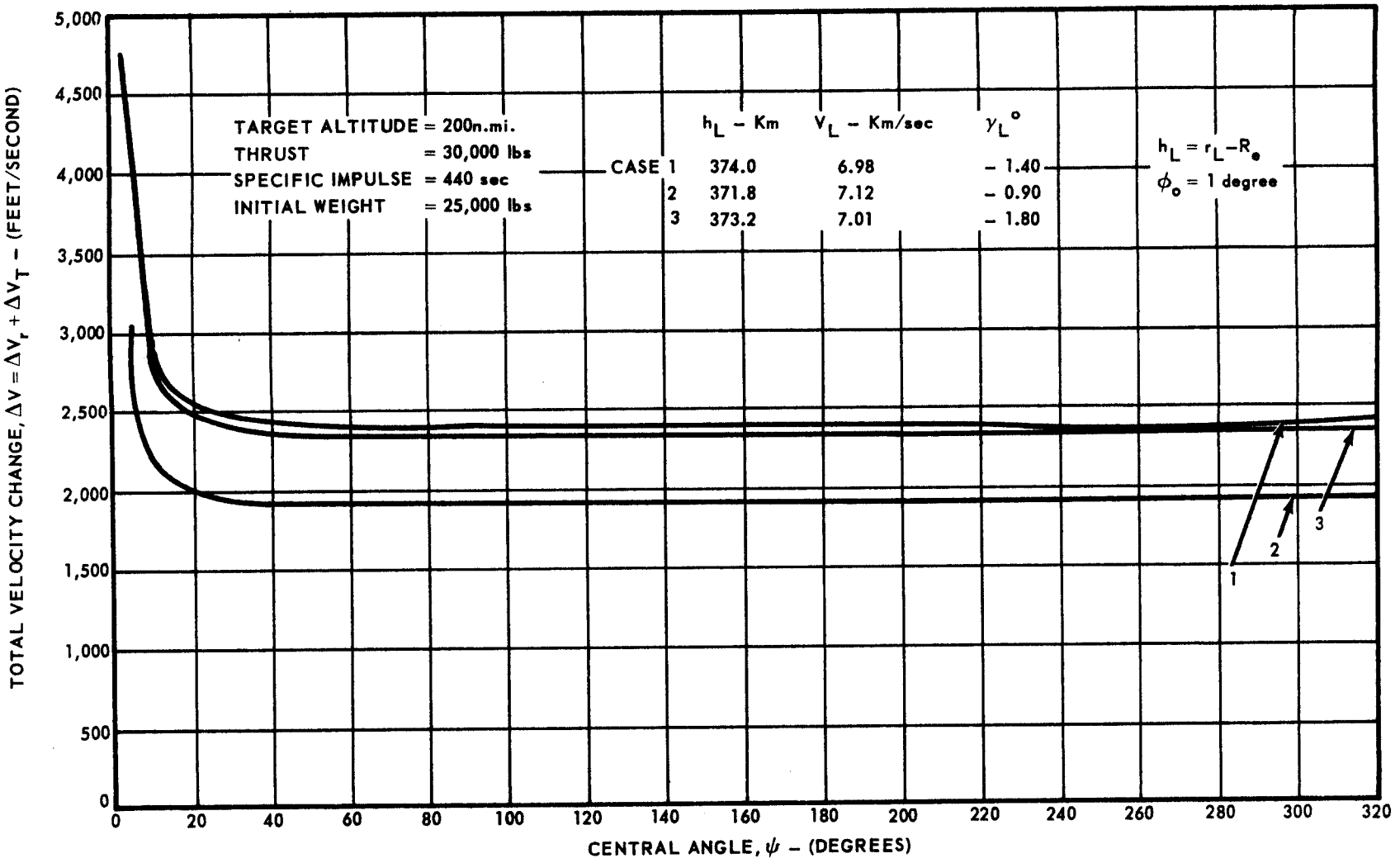

Figure C-5 Velocity Change as a Function of Central Angle

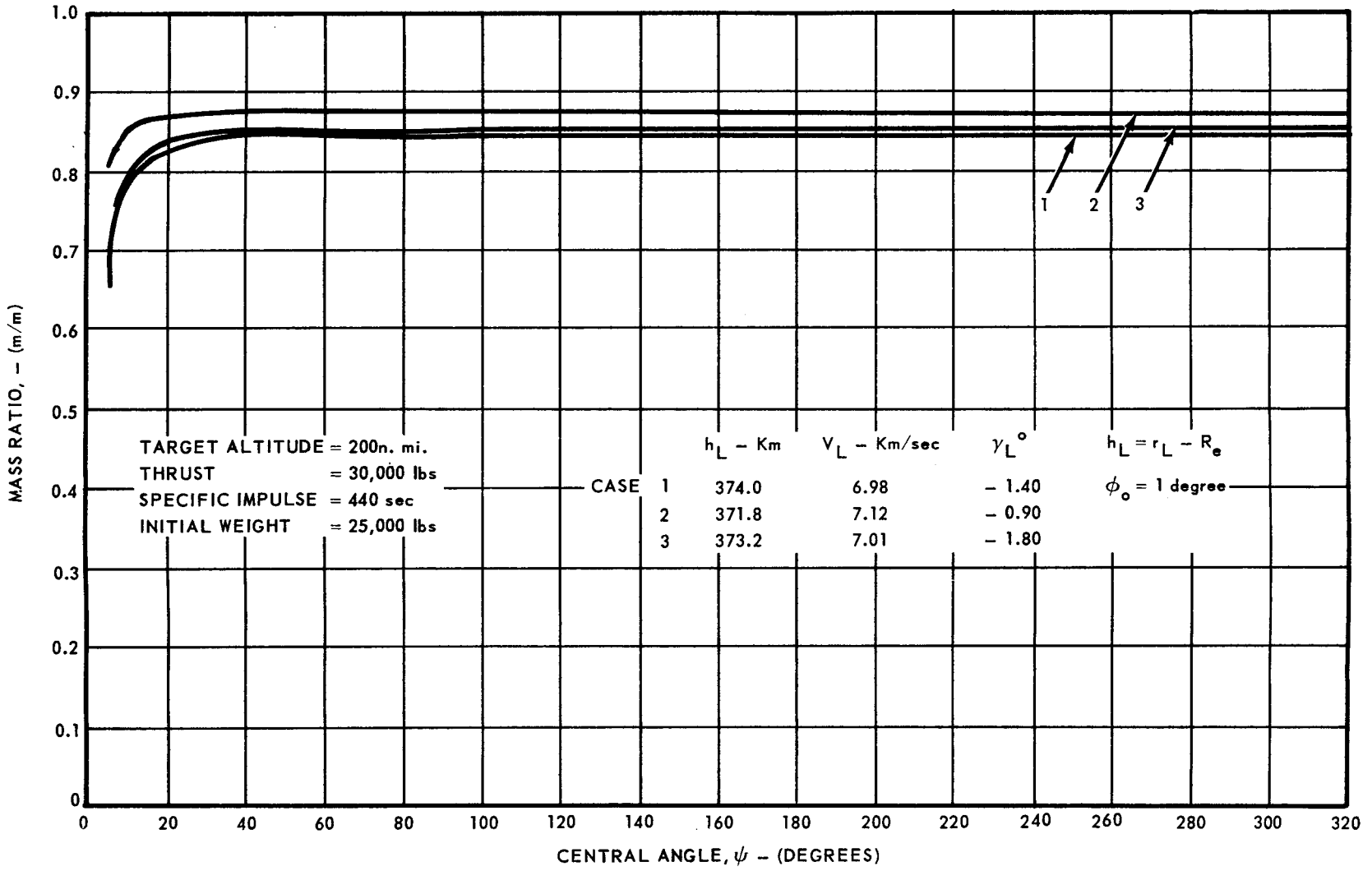

Figure C-6 Mass Ratio as a Function of Central Angle

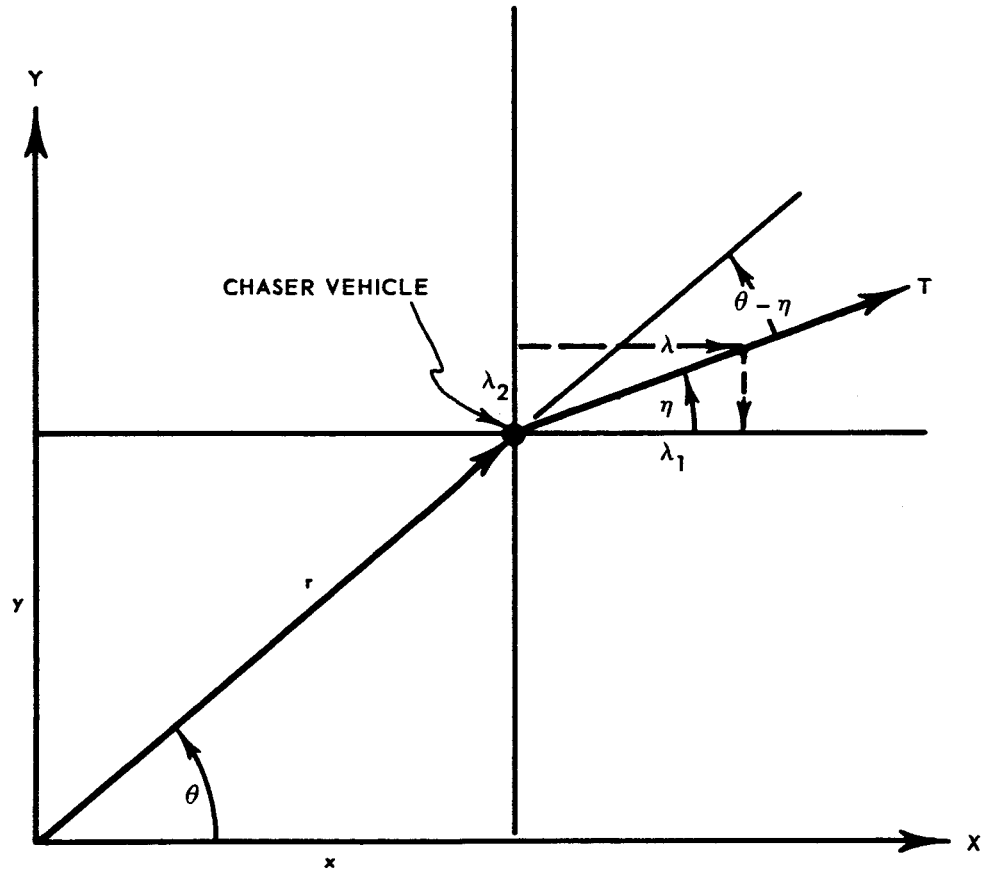

Figure C-7 Rendezvous Geometry in Polar Form

These quantities are related to those in Section 2 follows:

$$\lambda_1 = \lambda \cos \eta$$

$$\lambda_2 = \lambda \sin \eta$$

$$X_1 = r \cos \theta$$

$$X_2 = r \sin \theta$$

$$\tan X_p = -\tan \eta$$

The relationship between Γ and λ_5 is given by

$$\Gamma = \frac{V_e}{m} \lambda - \lambda_5 - 1 \qquad (4\text{-}2)$$

so that an initial value of Γ is equivalent to an initial value of λ_5.

The investigation of the effects of the initial conditions were carried out in the following manner. Initial conditions on r, θ, $\dot{r}$, and $\dot{\theta}$ are given. Since Equations (4-1) are homogeneous in λ, the initial value of λ is immaterial to the trajectory. In order to approximate the two impulse case, a good guess of the initial value of η is the value of β_L determined in Equation (3-7), and $\dot{\lambda} = 0$, $\dot{\eta} = \dot{\theta}$ initially. To observe the effects of these parameters, Equations (4-1) are integrated numerically, assuming that the thrust engine is on initially, i.e., T = 0.

At each instant of time, the transfer orbit that would result if thrust were terminated at that instant is computed. Thus, instantaneous transfer orbits are generated. These transfer orbits are shown in Figure C-8.

At time t, the values of r, $\dot{r}$, θ, and $\dot{\theta}$ known from the integration of Equations (4-1). Then the semi-major axis, semi-latus rectum, and true anomaly of the instantaneous tranfer orbit are found from the following equations:

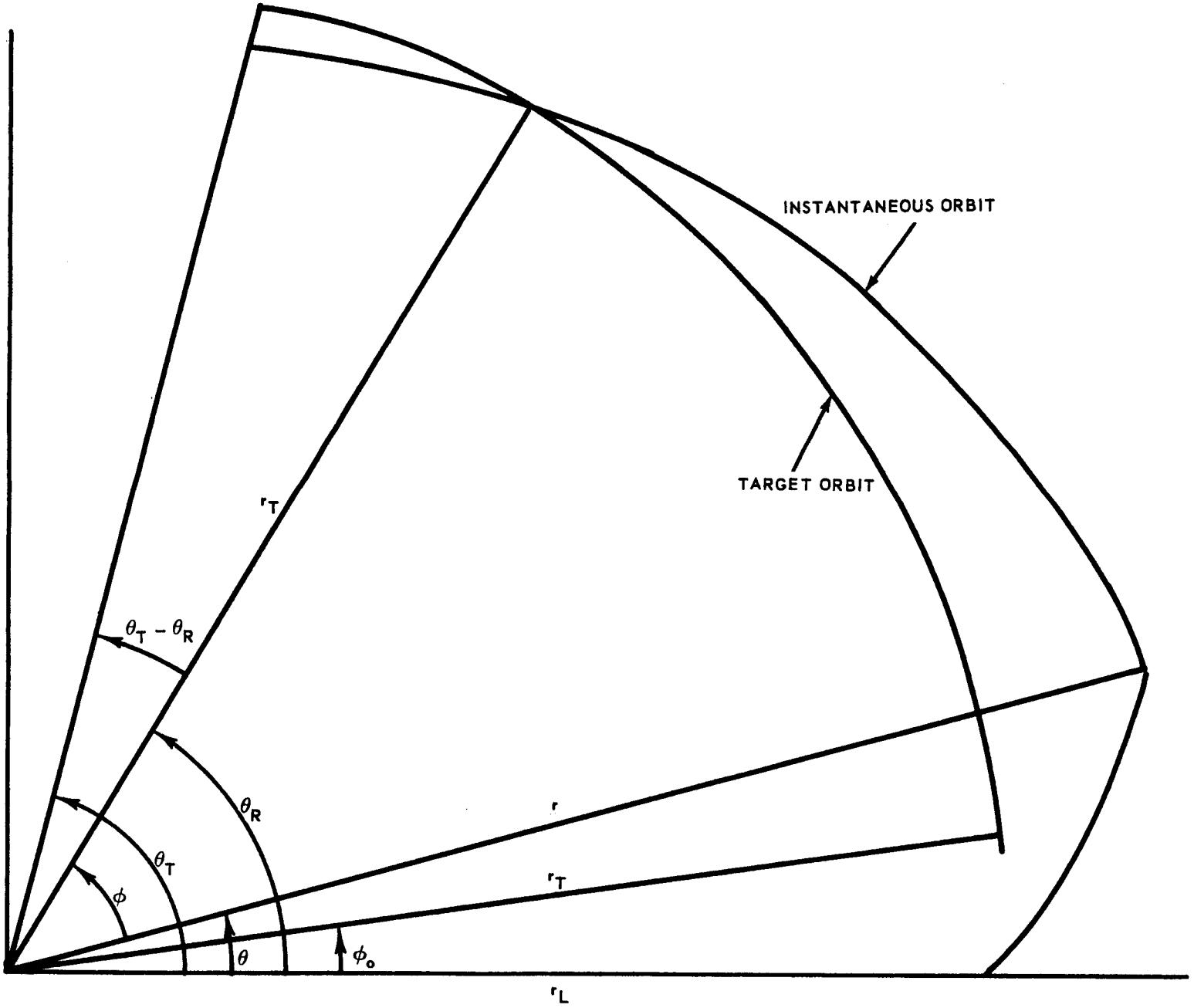

Figure C-8 Instantaneous Transfer Orbit Geometry

$$a = \frac{r}{2 - r V^2/k} \tag{4-3}$$

$$p = (r^2 \dot{\theta})^2/k \tag{4-4}$$

$$e \cos v = \frac{p - r}{r}$$
$$e \sin v = \frac{r^2 \dot{r} \dot{\theta}}{k} \tag{4-5}$$

This transfer orbit intersects the target when $r = r_T$. Let ϕ be the central angle subtended between the position at time t and the point where the instantaneous orbit crosses the target orbit. This angle is given by

$$e \cos (v + \phi) = \frac{p}{r_T} - 1$$
$$e \sin (v + \phi) = \text{sign} (r_T - r) \sqrt{e^2 - e^2 \cos^2 (v + \phi)} \tag{4-6}$$

To relate this to time of flight, the eccentric anomaly of the instantaneous orbit is computed as follows:

$$\cos E = \frac{(e^2 + e \cos v)\, r}{e\, p}$$
$$\sin E = \frac{r\, e \sqrt{1-e^2} \sin v}{e\, p} \tag{4-7}$$

When the orbit intersects the target orbit:

$$\cos E_T = \frac{\left[e^2 + e \cos (v + \phi)\right] r_T}{e\, p}$$
$$\sin E_T = \frac{r_T e \sqrt{1-e^2} \sin (v + \phi)}{e\, p} \tag{4-8}$$

Therefore, from Kepler's equation, the time interval corresponding to the orbit from E to E_T is given by:

$$\Delta t = \sqrt{\frac{a^3}{k}} \left[(E_T - E) - e (\sin E_T - \sin E) \right] \qquad (4\text{-}9)$$

The angular position of the target when the instantaneous orbit intersects the target orbit is given by:

$$\theta_T = \phi_0 + (t - \Delta t) \sqrt{\frac{k}{r_T}} \qquad (4\text{-}10)$$

The angular position of the chaser at this time is:

$$\theta_R = \theta + \phi \qquad (4\text{-}11)$$

Thus the angular error is given by:

$$\Delta\theta = \theta_T - \theta_R \qquad (4\text{-}12)$$

These quantities are computed at each time t as the differential equations are integrated. Intercept occurs if thrust is terminated when $\Delta\theta = 0$. If Γ is initially set equal to zero, then letting

$$\Gamma_0 = - \int_0^t \dot{\Gamma} \, dt$$

will cause the thrust to terminate at this instant. By varying $\dot{\lambda}_0$, η_0, $\dot{\eta}_0$, corresponding values of Γ_0 are obtained for intercept.

5.0 INTERCEPT CONDITIONS

In order to evaluate the effects of small variations in the initial conditions on intercept, the equations of motion were integrated in relative coordinates to eliminate the numerical difficulties inherent in dealing with orbits that are close together. Therefore, the following equations were used. First define

$$\xi = X_1 - X_{1T}$$

$$\zeta = X_2 - X_{2T} \tag{5-1}$$

where

$$X_{1T} = r_T \cos\left(\sqrt{\frac{k}{r_T^3}}\, t + \phi_0\right)$$

$$X_{2T} = r_T \sin\left(\sqrt{\frac{k}{r_T^3}}\, t + \phi_0\right)$$

Then the differential equations of motion of Section 2.0 become:

$$\ddot{\xi} = \frac{T'}{m} \cos\eta + \frac{k}{r_T^3}(X_1 f - \xi)$$

$$\ddot{\zeta} = \frac{T'}{m} \sin\eta + \frac{k}{r_T^3}(X_2 f - \zeta) \tag{5-2}$$

where

$$f = 3q\left(1 - \frac{5}{2!}q + \frac{5.7}{3!}q^2 - \frac{5.7.9}{4!}q^3 + \ldots\right) \tag{5-3}$$

$$q = \frac{1}{r_T^2}\left[\left(X_{1T} + \frac{1}{2}\xi\right)\xi + \left(X_{2T} + \frac{1}{2}\zeta\right)\zeta\right]$$

$$T' = - \text{ when } \Gamma < 0$$

$$T' = T \text{ when } \Gamma \geq 0 \tag{5-4}$$

and $\ddot{\lambda}$ and $\ddot{\eta}$ are defined in Equations (4-1).

These equations were integrated using initial values obtained by the methods described in Section 4.0, and small variations were made. The trajectories were run until target-chaser distance

$$d = (\xi^2 + \zeta^2)^{1/2}$$

went through a minimum. As was expected, this miss distance was extremely sensitive to initial conditions on the Lagrange multipliers. On the other hand, small variations cause very small variations in firing time, and hence have a negligible effect on fuel consumption.